UCSF
UC San Francisco Electronic Theses and Dissertations

Title
Network Dynamics in the Hippocampus during Spatial Learning

Permalink
https://escholarship.org/uc/item/17f962hw

Author
Karlsson, Mattias

Publication Date
2008-09-08

Peer reviewed|Thesis/dissertation

eScholarship.org Powered by the California Digital Library
University of California

Network Dynamics in the Hippocampus during Spatial Learning

by

Mattias P. Karlsson

DISSERTATION

Submitted in partial satisfaction of the requirements for the degree of

DOCTOR OF PHILOSOPHY

in

NEUROSCIENCE

in the

GRADUATE DIVISION

of the

UNIVERSITY OF CALIFORNIA, SAN FRANCISCO

To

my parents Kerstin and Magnus,

my wife Ellie,

and my son Linus.

Acknowledgements:

For support and ideas

Margaret Carr, Sen Cheng, Yuri Dabaghian, Sheri Harris, Caleb Kemere, Steve M. Kim,

Ana R. Nathe, Annabelle Singer, Ken Park, Mel Wohlgemuth, and Hillel Adesnik

For mentorship

Loren Frank, Flip Sabes, Michael Brainard, Steve Lisberger, and Michael Stryker

Abstract

The hippocampus is essential for encoding new memories for space and events. In the rodent hippocampus, a result of this process is that individual neurons fire selectively when the animal is located in a particular subregion of its environment. We show that that hippocampal area CA1, but not upstream area CA3, emits twice as many spikes in novel as compared to familiar environments, and during the initial stages of novelty many CA1 neurons are active. The overall population rate and the number of active cells decreases as the environment becomes familiar, but the decline in rate is not uniform across neurons. Instead, the activity of cells with peak spatial rates above ~12 Hz is enhanced, while the activity of cells with lower peak rates is suppressed. The result is that, after several days of experience in the environment, the active CA1 population consists of a relatively small group of cells with strong spatial tuning. This process is not evident in CA3, suggesting that a region specific selection process operates in CA1 to create a sparse, spatially informative population of neurons. We also show that there is clear and long lasting replay of experiences from one place during waking behavior in subsequently experienced places. Surprisingly, this remote replay was most robust when the animal had recently been in motion as compared to during extended periods of immobility. These results indicate that waking and sleep replay both constitute a form of memory retrieval where past experiences can be reactivated, and that patterns of activity associated with memory consolidation continue unabated during both sleep and awake states.

Table of Contents

Overview…….1-3

Chapter 1

Introduction…….4-5

Results…….5-13

Discussion……...13-19

Methods……...19-25

Figures…….26-42

Chapter 2

Introduction……..43-44

Results……..44-53

Discussion…….53-57

Methods…….58-63

Figures……...64-75

Notes……..76-80

Overview

The hippocampus is a brain area that is integral to the process of learning and memory— it is necessary for the formation of memories in both humans and animals [1-3]. Damage to the hippocampus in humans degrades the ability to retain new semantic memories[1], and lesion studies in rodents have shown that the hippocampus is required for normal spatial memory [4, 5]. The hippocampus is most crucial during the initial formation of a memory; after a gradual *consolidation* period, it ceases to be necessary for most memory recall. It is believed, therefore, that the neural circuitry of the hippocampus may be specialized for fast neural plasticity, allowing it to be the initial storage site for ongoing experiences. The newly learned information may then be slowly transferred to slower learning cortical networks for more permanent storage.

While this theory is largely based on lesion work, recent electrophysiological studies also suggest that the hippocampus is important for encoding and consolidating new memories. Many of these studies are based on the finding that neurons in the hippocampus are responsive to the animal's location [6, 7]. Such 'place cell' activity has been proposed to represent a cognitive map of the environment, and it transitions from a state of inconsistent spatial selectivity to a highly stabilized set of 'place fields' as an animal explores a novel environment [8, 9]. Much of this stabilization occurs during the first few minutes of exploration, and it is thought to occur as the animal builds a representation of its surroundings. The place cell phenomenon therefore serves as a useful tool for studying plasticity and learning in the hippocampus of behaving animals.

For both chapters presented in this thesis, we present neural recordings from place cells in hippocampal subregions CA1 and CA3. Evidence from anatomical, genetic, and place cell studies strongly suggest that these subregions perform different roles during memory formation[10-12], but the nature of these specializations is not well understood. CA3 pyramidal neurons are highly interconnected[13], which may allow the subregion to function as an attractor network with efficient recall and learning mechanisms[14-17]. Modeling studies also suggest that CA3 is specialized for recalling sequences of events[16, 18], making it important for predicting future events based on history. CA3 sends projections to CA1, which in turn sends projections to the cortex, subiculum, and subcortical areas. CA1 therefore serves as the primary output of the hippocampus.

The first chapter focuses on neural dynamics during the encoding of new memories. We show that that hippocampal area CA1, but not upstream area CA3, emits twice as many spikes in novel as compared to familiar environments, and during the initial stages of novelty many CA1 neurons are active. The overall population rate and the number of active cells decreases as the environment becomes familiar, but the decline in rate is not uniform across neurons. Instead, the activity of cells with peak spatial rates above ~12 Hz is enhanced, while the activity of cells with lower peak rates is suppressed. The result is that, after several days of experience in the environment, the active CA1 population consists of a relatively small group of cells with strong spatial tuning. This process is not evident in CA3, suggesting that a region specific selection process operates in CA1 to create a sparse, spatially informative population of neurons.

In the second chapter, we focus on hippocampal consolidation. It is widely believed that the formation of long-term memories relies on replay of recently

stored hippocampal information after the original experience has passed. This replay process is thought to be most robust during sleep following the experience, but we do not yet know whether memory replay is restricted to sleep-like states. Here we show that there is clear and long lasting replay of experiences from one place during waking behavior in subsequently experienced places. Surprisingly, this remote replay was most robust when the animal had recently been in motion as compared to during extended periods of immobility. These results indicate that waking and sleep replay both constitute a form of memory retrieval where past experiences can be reactivated, and that patterns of activity associated with memory consolidation continue unabated during both sleep and awake states.

Chapter 1

Network dynamics underlying novelty signaling and the formation of sparse, informative representations in the hippocampus

Introduction

The hippocampus is essential for encoding new memories for space and events [1, 19, 20]. In the rodent hippocampus, a result of this process is that individual neurons fire selectively when the animal is located in a particular subregion of its environment [6]. These "place cells" encode complex associations among the various types of information available to the animal in different locations [21]. Importantly, not all hippocampal place cells are active in a given environment. Instead, about 40% of the principle neurons in hippocampal area CA1 and about 30% of the principle neurons in upstream area CA3 [8, 12, 22] show clear spatial specificity in a given familiar environment while the rest are essentially silent. It is not yet clear how individual neurons are selected to be part of a new spatial representation or whether the same process operates in CA1 and CA3.

We do know that there are increases in activity across multiple brain regions during exposure to novelty [23-26] suggesting that increases in activity may be important for the processing of new information. In the hippocampus these increases have been found in area CA1, in that CA1 neurons become more active when animals explore new environments [27, 28], but we do not yet know whether these changes are present in CA3. In any case, these increases in overall rate suggest that the CA1 network is in a more permissive state during learning, allowing more neurons to contribute to network activity.

If so, then the dynamics of neural activity as the network returns to a less permissive state may provide important information about how cells are selected for persistent membership in a long-lasting memory.

Any differences between CA3 and CA1 may also help us identify the specific contributions of each of these regions to spatial memory storage. We know that place cells in CA1 and CA3 respond differently to environmental manipulations[12, 22, 29, 30]. Further, plasticity in CA3 has been implicated in the rapid storage of one time experiences [11]. The specific role of CA1 remains unclear, however. In an effort to understand how individual neurons are incorporated into long lasting representations and how this process might differ between CA1 and CA3, we recorded hippocampal place cell activity across many days as rats explored initially novel environments that became increasingly familiar. We found fundamentally different patterns of population dynamics in CA3 and CA1 suggestive of specialized roles for these structures in memory formation.

Results

. Each recording day consisted of two or three 15-minute 'run' sessions in W-shaped tracks, with 'rest' sessions in a black box before and after each run. We used two geometrically identical but visually distinct tracks that were open to the room but separated from one another by a black barrier (Fig. 1a). We isolated large numbers of neurons on each day from both CA1 (total n = 708) and upstream area CA3 (total n = 984) which provides direct synaptic input to CA1 (Fig. 1b, Fig. 2a, Supplemental Fig. 1). As expected [31, 32], we were able to maintain stable recordings across each day (Fig. 2c)

and animals created distinct spatial representations of the two tracks in both areas, indicating that the animals formed unique representations for each environment (Fig. 2b ,d). Only a small number of putative inhibitory neurons were recorded, so we did not include data from these neurons in this study.

CA1-specific rate dynamics

We first sought to characterize the timeline of the previously observed increase in CA1 activity during novelty. We compared absolute firing rates across the two tracks for animals in group 1 and found that CA1 neurons were on average more active on the more novel T2 (paired $t(145) = 2.04$, $p < 0.05$), a result consistent with previous studies. Using recordings across multiple sequential days, we were able to quantify the decay of the rate change. For every recording session, we calculated the average firing rates of all recorded CA1 principle neurons, including those that fired very few spikes on the tracks, and combined these rates into an estimate of the population average rate. We included all clustered principle neurons rather than imposing a cutoff because we wanted to minimize the selection bias for the measure of population activity. Rates slowly declined across multiple days of experience (T1, $R^2 = 0.026$, slope ± 95% bounds = -0.29 ± 0.2 Hz/day, $p < 0.005$), indicating a long timescale process rather than a transient response to novelty.

The same dynamics were observed in recordings from group 2 (Fig. 3a, right). Again, CA1 activity was initially high in the more novel T2 and slowly decreased over multiple days of exposure ($R^2 = 0.023$, slope = -0.33 ± 0.22 Hz/day, $p < 0.005$), while activity on the more familiar T1 was lower on all recording days (paired $t(457) = 4.96$, $p < 10^{-6}$) and did not decline appreciable with further experience. We should note that

although we used a linear regression to quantify the decline in slopes, the rates from group 1, track 1 and group 2, track 2 appear somewhat sigmoidal, while the rates from group 1, track 2 are more linear or exponential in character. The large variability in mean rates makes it difficult to determine the exact shape of these curves, but it is nevertheless clear that there is a substantial decrease in rate over time. Furthermore, because the rate difference is observed both within single recording sessions and across days, the effect is unlikely to be due to within-day confounds such as environment sequence or cell isolation instability, or across-day confounds such as quantity of recorded cells or tetrode placement. Furthermore, none of the potential behavioral confounds we examined, including differences in velocity, head direction, or ripple-related activity in the local field potential, could explain these results (Supplemental Fig. 3).

The increase in rate was not present one synapse upstream in CA3 (Fig. 3b). CA3 neurons had on average lower activity than CA1 for most recording days, and unlike neurons in CA1, did not show a consistent decline in activity as the environments became more familiar (linear regression, both groups, N.S.). We compared the activity of single CA3 cells across the two tracks and found no significant difference in activity for either group ($t(185) = 0.1$, $t(612) = 1.54$, N.S.). Thus, unlike in CA1, no significant population rate change was observed in CA3 either within or across days. These results indicate that the change in CA1 was not due to inheritance of higher rate activity from CA3.

We pooled data from both groups of animals and found that CA1 as a whole emits more than twice as many spikes per second in a novel as compared to a more familiar environment (Fig. 3c). Here, ‘day 1’ represents the combined data across all animals from the first day of exposure to each track. CA1 population activity during initial

exposures was ~ 0.9 Hz per neuron as compared to ~ 0.4 Hz observed during more familiar exposures, and the majority of the rate decline occurred during the first 5 days of exposure to an environment. When we pooled CA3 neurons across all animals, we found that population rates were flat, averaging about 0.3 Hz across all exposure days (linear regression, N.S.).

Changes in CA1 activity were associated with the initial recruitment of a large fraction of CA1 neurons and the subsequent reduction in the number of active cells. We divided our data into three blocks—early (days 1-2), middle (days 3-6), and late (days 7-14)—to provide accurate estimates of the initial, intermediate, and stable periods of the rate curve (Fig 3c, top). We then counted the number of active neurons out of the total number of isolated neurons, once again including cells that were active on the track and cells that were inactive on the track but could be isolated in the rest sessions before and after the behavior. We applied a 0.1 Hz mean rate threshold to designate active neurons and found that 151/275 (55%) of cells were active in the early novelty block and 203/406 (50%) in the middle block while only 239/600 (40%) were active in the late block (early vs. late, $Z = 4.20$, $p < 10^{-4}$; note: some cells provided data for both tracks 1 and 2, which in turn provided data for two novelty blocks). There was no evidence for similar changes in CA3, where the proportion of active cells was constant across the three novelty blocks, with 108/373 (29%), 185/591 (31%), and 234/776 (30%) active (early vs. late, $Z = 0.42$, N.S.).

Network selection of cells with strong spatial tuning

We then asked whether the specific tuning properties of individual CA1 place cells influence whether or not they are silenced. We examined the proportion of the track on which each neuron was active and found that this proportion tended to decrease as environments became familiar (ranksum, median early block proportion = 0.08; median late block proportion = 0.03, $p < 10^{-3}$), indicating that spatial activity became more focused with experience. This trend persisted when we considered only cells with substantial spatial activity (peak spatial rate of at least 5 Hz, ranksum, median early block proportion = 0.30; median late block proportion = 0.22, $p < 0.005$).

One might expect that the overall decrease in both total firing and in the spatial extent of activity was a result of an overall suppression of activity in CA1. In actuality, however, the population of active place cells showed an enhancement of spatial firing over time. We examined the relationship between the proportion of the environment on which each neuron was active and the peak activity within each cell's place field (Fig 4a, Supplemental Fig. 4). In the early block (open blue circles; blue line), many CA1 cells were active across large fractions of the environment, yet tended to have low peak spatial rates. As the environment became familiar (middle block, dotted line and late block, filled black circles; dashed black line), the CA1 population segregated into two groups: a large group of neurons with low peak rates and a smaller group of cells with high peak rates. Both of these groups were active in smaller proportions of the environment than in similar groups from the early block and the slopes of regression fits to the data showed a significant decline with experience (block 1 vs. 2, $p < 0.0001$; block 2 vs. 3, $p < 0.02$). This segregation suggests that the peak spatial firing rates tend to move toward the extremes of either low or high rate activity.

We plotted the distribution of peak spatial rate for each of the three novelty blocks to assess the magnitude of this effect. We found clear differences in the distribution across novelty blocks (early vs. middle, Komolgorov-Smirnov (KS) test, $p < 0.05$; early vs. late, $p < 0.001$, Fig. 4b). The three novelty block distributions intersected at two central points, providing a natural grouping of peak spatial rates. Using this grouping we compared the early and late blocks and found that the proportions of cells with intermediate peak rates decreased by about half (5 - 25Hz, $Z = -4.56$, $p < 10^{-6}$; Fig. 4c). This decrease was associated with a redistribution of neurons into both the high peak rate and low peak rate groups (Fig. 4d), resulting in more than a doubling of the proportion of neurons (from 7% to 17%; $Z = 3.1$, $p < 0.01$) in the high peak rate group and equal magnitude increase (from 55% to 65%, $Z = 2.0$, $p < 0.05$) in the low peak rate group. This segregation into two rate groups suggests that the activity of some neurons with intermediate peak rates is enhanced, while the activity of others is suppressed.

Importantly, there was no evidence for such dynamics as a function of average rates across the run session. We examined the distribution of average rates for the cells in the early, middle and late novelty block and found that, other than the expected shift toward lower rates, there were no other systematic changes in the distributions (Fig. 5). This shows that the segregation process is not simply based on the total activity of the cells, but instead favors cells with strong, spatially localized activity. Furthermore, the changes across the novelty blocks differed in CA3. The linear regression on the scatter plots of peak rate versus proportion active showed a significant decrease in slope from the early to the middle block but no subsequent change between the middle and late blocks (Fig. 6a). An inspection of this plot makes it clear that there were only relatively

modest changes, in that cells remained active across large fractions of the track in both the early and the late blocks. Furthermore, there was no obvious increase in the number of high peak rate neurons. Instead, the peak rate distributions of CA3 neurons changed only slightly, with a decrease in the proportion of peaks near zero and a slight increase in the proportion of high rate cells (KS test, early vs. middle, N.S, early vs. late, $p < 0.05$; Fig. 6b.).

What governs whether a CA1 cell's peak activity is enhanced or suppressed? If it depends on the current peak rate of the cell, one might expect to see a transition point within the 5-25 Hz peak rate range, where the peak spatial rate of cells with rates below the transition point will tend to decrease, while the peak spatial rate of cells with rates above it tend to increase. Ideally, one would record from the same cell across many days to accurately describe this relationship, but as it is very difficult to conclusively demonstrate that the same neurons were recorded across days, we instead analyzed the dynamics of neurons within single recording sessions. We reasoned that if the place field changes are due to a single continuous process, the dynamics of single neurons within a day should be sufficient to predict the changes in the population across days. All animals were exposed to either T1 or T2 twice a day, so we were able to measure differences in activity of single neurons across consecutive runs in an environment. For each cell, we compared the peak spatial rate on the first run to the subsequent within-day change in peak spatial rate. Strikingly, cells in the 5-25 Hz range showed a sharp transition between about 6 and 18 Hz: the peak spatial rate tended to decrease for cells with initial rates < 12 Hz and increase for cells with initial rates > 12 Hz (Fig. 7a). We calculated the likelihood of this transition appearing by chance by shuffling the peak rate / peak rate

change relationships for cells in the intermediate group 5000 times and calculating how often a transition whose peak and trough value exceeded those we measured occurred by chance. We found that this sharp transition was unlikely to arise by chance ($p < 0.01$). These within day dynamics strongly support the claim that the activity of place cells tends to be either enhanced or inhibited based on the strength of spatial tuning. The highly selective nature of these changes also argues against any behavioral explanation for the CA1 results, as there is no evidence for behavioral modulations that affect cells differentially as a function of peak spatial firing rates.

The derived curve represents a system that evolves toward two stable fixed regions. This is illustrated by a cartoon of the associated energy surface (Fig. 7b) which has one low energy region near zero and another above 20 Hz. To identify the final state of a network that evolves according to this rule we used the actual within day changes from the middle block to simulate the across day evolution of the early block population (Supplemental Fig. 2). We found that the rate distribution became increasingly different from the initial distribution and converged after about 100 iterations (Supplemental Fig. 5). The resulting simulated population distribution was similar to the actual late block distribution and had two main peaks: one centered near zero and the other centered at 31 Hz (Fig. 7c). Compared to the early block, the proportion of cells with peak spatial rates below 5 Hz increased ($Z = 4.59$, $p < 10^{-5}$), the proportion between 5 and 25 Hz decreased ($Z = 6.98$, $p < 10^{-11}$) and the proportion above 25 Hz increased ($Z = 4.06$, $p < 10^{-4}$). This pattern did not arise when we performed the same simulations using randomly scrambled peak rate – rate change relationships from the middle block (Supplemental Fig. 6). Thus, using within day changes, we were able to identify the main pattern of dynamics in the

CA1 network and then use these dynamics to predict the actual changes that occur over the course of many days of experience.

To test if the simulated change in the peak rate distribution predicts the observed decrease in population activity, we made the conservative assumption that the mean rate of each cell changes proportionately to the peak rate. This assumption ignores dynamics related to the sharpening of place fields, where out-of-field rates decrease faster than within-field rates, and therefore likely causes an underestimate of the magnitude of decrease. Nonetheless, the simulation predicted a decrease in the mean population rate (from 0.84 Hz to 0.62 Hz, ranksum $p < 10^{-5}$). As might be expected given the numerous factors that are likely to govern neural dynamics across days, the precise quantitative outcomes of the simulation and the actual data were not identical. Despite this, the types of changes seen were very similar. Thus, a rule that selectively suppresses neurons with low spatial specificity and preserves neurons with high spatial specificity captures the key properties of the long term plasticity seen in the CA1 population.

Finally, we asked whether the differences in firing rate during a run session carried over to a subsequent rest session. We computed the firing rates of all CA1 and CA3 principle neurons during sharp wave (SWR) events that occurred while the animals was in the rest box following the first run of each day. We found that the rate changes we saw from early to middle to late blocks during the runs carried over to SWR events in the rest session (Fig. 8). CA1 cells showed a clear decline in rate associated with greater experience in the novel track (ranksum, early vs. middle $p < 0.02$, early vs. late, $p < 10^{-4}$) ,while the rates of CA3 cells remained constant (ranksum, p's > 0.1).

Discussion

We have shown that spatial learning in hippocampal area CA1 invokes a plasticity mechanism that selects a subset of the initially active neurons to remain as part of a longer lasting representation. During the initial exposure to a novel environment, many CA1 cells are active and the population as a whole produces more than twice as many spikes as in a familiar environment. This occurs both within the novel environment and during SWRs in a separate rest box. This increase is greater than that seen previously [27, 28], perhaps because we included all recorded neurons rather excluding lower rate neurons based on a chosen cutoff. On average, the spatial activity of individual neurons is relatively diffuse during this high rate period. Over time the population firing rate decreases to familiar levels. This is due to a decrease in the proportion of active cells and because cells that remain active tend to retain activity only in focused areas of the environment. In the midst of this global suppression, however, the place fields of some neurons undergo an enhancement of activity. A simple rule can be derived from within-day changes governs the subsequent dynamics: cells that are weakly spatially tuned are suppressed while strongly spatially tuned activity is enhanced. The result is a large group of minimally active neurons and a smaller group of well tuned cells with high peak spatial firing rates. The same process is not evident one synapse upstream in CA3, where the same fraction of neurons is active throughout the animal's experience and there is no evidence for selection based on spatial tuning.

These results cannot easily be explained by any known behavioral modulations of place cell activity. The increases in CA1 population rates were not a result of low velocities, differences in head direction or activity during ripples. Further, previous

results have demonstrated that CA1 firing rate is positively correlated with velocity[33], which predicts that rates would be lower during initial, low velocity exploration of a novel environment. Thus, our results are the opposite of what would have been expected from the known velocity dependence of place cell firing. Second, the fact that these changes were not present in CA3 implies that any potential behavioral affect would be one that affects only CA1 and not CA3, and to our knowledge no such effect has been reported.

Previous work demonstrated that reconstructions of an animal's position based on place cell firing become more accurate over a 10 – 20 minute time course of experience in a new place[8], and that CA1 place fields undergo rapid plasticity when an animal enters a new environment[9, 12]. These papers suggested that place field plasticity ended after at most one to two days of experience in the new place. Our results indicate that there is another, slower process that continues after the initial rapid formation of place fields. We found alterations in rate and spatial specificity between the middle and late novelty blocks, indicating that the hippocampal representation was dynamic for at least 4–6 days, even though the animal experienced the novel environment twice a day. While longer timescale changes have been observed in the context of exposure to multiple similar environments[34] we are not aware of any previous results documenting these sorts of changes within a single static environment.

Overall, the active selection of high peak spatial firing rate neurons is conceptually similar to the sorts of activity dependent plasticity that increase the specificity of neural tuning during development[35]. That said, our finding is, to our knowledge, the first demonstration that the strength of tuning differentially modulates

changes in neural activity during the formation of representations in the adult. The fact that CA1 appears to select for high absolute spatial firing rates calls into question previous approaches that treat all place cells equivalently. Most work in the place cell field, and indeed many other fields, uses a cutoff to select a set of active cells and then analyzes the activity of each neuron individually[21]. The result is that when measures from multiple neurons are combined, each neuron contributes equally to the final result. The implicit assumption behind this approach is that the activity of a cell with a peak rate of 3 Hz is as meaningful to the system as the activity of a cell with a peak rate of 40 Hz. Our analyses show that the dynamics of CA1 do not treat cells with different peak spatial rates equivalently, but instead favor high peak rate neurons. This suggests that a higher peak spatial rate cell is better able to represent and transmit spatial information than a lower rate cell, and more generally that absolute firing rates may be important.

What mechanism could account for the CA1 specific changes we observed? Previous work has established that the firing rate of CA1 interneurons drops in novel environments[27] and then increases as the environment becomes more familiar[9]. A decrease in inhibition could certainly contribute to the initially high rates in CA1 and a subsequent increase in inhibition could play a role in the decrease in CA1 principle cell activity. At the same time, a simple increase in inhibition would be expected to decrease the firing of all principle neurons, and thus cannot account for the selective increases in peak spatial rate seen for neurons with peak rates between about 12 and 18 Hz and the preservation of neurons with peak rates greater than 18 Hz. It is therefore likely that some other process, likely one involving synaptic plasticity, is involved.

One candidate for such a process was discovered recently in the amydgala. Han et. al. [36] showed that levels of CREB seen during the initial encoding of a fear memory were predictive of which neurons would participate in the memory during a subsequent retrieval as measured by expression of the immediate early gene Arc. Higher initial levels of CREB during encoding were associated with higher probabilities of activity during retrieval. Thus, high activity during encoding predicted membership in a long lasting memory, a pattern of results very similar to those reported here. Given that neural activity leads to CREB expression [37], we suggest that the amygdala and CA1 may employ similar mechanisms to select highly informative neurons to participate in mnemonic representations.

Increases in activity as a result of exposure to new stimuli have also been seen in electrophysiological and imaging studies focused on other brain areas[23-26], suggesting that numerous brain increase their activity the development of representations for new stimuli. We may then wonder why CA3 activity does not show a similar high firing rate state during the initial stages of spatial learning. We suggest that CA3's relatively stability, both in the context of firing rates and in the context of place fields which did not change from the middle to the late novelty blocks, is a result of CA3's role in the rapid formation of new representations [11]. We know that CA3 place fields shift during the first exposure to a new cue configuration but not during subsequent exposures [30], suggesting that CA3 plasticity can be rapid. We therefore hypothesize that CA3 develops spatial representations quickly and shows only minimal changes during subsequent experiences, thereby preserving the original representation.

These minimal changes in CA3 imply that CA1 receives approximately the same number of spikes from CA3 throughout the five to six days during which CA1 rates fall. In contrast, our results demonstrate that the subiculum and the entorhinal cortex (EC), the two main targets of CA1 outputs, will receive twice as many spikes from CA1 in a novel as compared to a familiar environment. Given that spikes are metabolically costly [38], this type of transient increase in neural output is likely to serve a functional role. Here we suggest a possible role for this substantial increase in CA1 spiking.

We propose that the high rate of spiking in CA1 could serve to both signal the presence of new spatial information and to facilitate plasticity in downstream structures. Theoretical models have suggested that CA1, by virtue of its inputs from CA3 and the EC, is well positioned to "compare" an internal hippocampal representation from CA3 with processed sensory information from the EC [39, 40]. These models predict that CA1 should be able signal the presence of a new representation from CA3 that is not yet associated with EC inputs, but the nature of that signal was not previously known. Our results show that higher firing in CA1 could signal the presence of new spatial information, a result that may also explain observations from human imaging studies of a hippocampal "novelty signal" whose strength is predictive of later recall [25, 41].

How then, would this information be used in downstream structures? One interesting possibility derives from evidence that novelty-dependent dopamine release in the nucleus accumbens requires hippocampal activity [42]. This suggests that increased CA1 output during both behavior and subsequent rest could trigger broadly distributed modulation that in turn could facilitate new learning across the brain. More generally, high rates in CA1 have the potential to increase the relative impact of CA1 firing on

downstream regions during behavior. Further, given the hypothesized association between SWRs and memory consolidation [43, 44], our results indicate that CA1 firing rates are also high during periods associated with the transfer of hippocampal representations to neocortical networks. Thus, we suggest that this greater total activity has the potential to increase the influence of CA1 on downstream structures during and after new experiences, potentially facilitating the consolidation process.

Methods

Data collection and pre-processing

Seven male Long-Evans rats (500-600g) were food deprived to 85 – 90% of their baseline weight and trained to run on a linear track with one reward site on each end of the track. The pre-training was performed in a different room from the recording experiments. After the animals were accustomed to behaving for liquid reward (sweetened condensed milk), they were implanted with a microdrive array containing 30 independently movable tetrodes according to UCSF and National Institutes of Health guidelines (see Frank et al. [9] for details). The tetrodes were arranged bilaterally in two 15 tetrode groups centered at at AP -3.7 mm, ML ±3.7 mm. Each group was located inside oval cannula whose major axis was oriented at a 45 degree angle to the midline with the front of the cannula closer to the midline. Tetrodes in the anterior portion and lateral portion of each group targeted lateral CA3 while more posterior and medial tetrodes targeted CA1. After 5-6 days of recovery, animals were once again food deprived to 85% of their baseline weight.

Each recording day consisted of two or three 15-minute 'run' sessions in W-shaped tracks, with 'rest' sessions in a black box before and after each run. We used two geometrically identical but visually distinct tracks that were open to the room but separated from one another by a black barrier (Fig. 1a). The tracks had one reward site at the end of each arm, and animals learned to performing a continuous alternation task where, starting from the center arm of the W-track, they alternated visits to each outer arm for liquid reward (center-left-center-right, and so on [9, 31]). Each outer arm visit was followed by a return to the center arm before the next outbound trajectory was made. Errors were not rewarded, and following an incorrect choice of an outer arm no rewards were given until the animal returned to the center arm. Recording for animals in group 1 (n = 4) began on the first day of exposure to track one (T1). These animals experienced T1 for three days (two sessions/day), and in three of these animals, track two (T2) was then introduced on day four. From day four onward these three animals ran at least one session on each track (usually two sessions on T2 and one session on T1. The fourth animal in group 1 ran only on track 1 for two sessions a day for days 1 through 5 and was not exposed to track 2. Animals in group 2 (n = 3) were exposed to T1 for six days and then ran on both T1 and T2 from days 7 onward. Recordings for group 2 were begun on day 7. A diagram showing the order of track presentations for each animal is shown in Supplemental Figure 1. The order of track presentations was not the same for every animal, but was kept consistent for each individual animal. This design allowed us to compare the activity of single neurons across the two tracks and to obtain recordings across many days as the initially novel environments became familiar.

Each run session was fifteen minutes long, and run sessions were flanked by 20 minute rest periods in a high walled black box where neural recording continued. Tetrode positions were adjusted after daily recording sessions for all tetrodes that had poor unit recordings. On rare occasions some tetrodes were moved before recording sessions, but never within four hours of recording. Following data collection electrode locations were identified histologically (see Fig. 1b. and Frank et. al. [9]).

Data were collected using the NSpike data acquisition system (L. Frank, J. MacArthur). The animal's position on the track was reconstructed using a semi-automated analysis of digital video of the experiment with custom-written software. After neural data was collected, individual units were identified by clustering spikes using peak amplitude and spike width as variables. Care was taken to only cluster well isolated neurons with spike waveform amplitudes that were clearly stable over the course of the entire session (Supplemental Fig. 1). All spike sorting was done using custom software (MatClust, M. Karlsson). Putative principle and inhibitory neurons were identified using standard firing rate and waveform characteristics and all analyses were restricted to putative principle neurons. Some cells were active only during rest sessions. These cells were included in the average rate analyses and in the calculation of proportion of cells active.

Analysis of neural data

All analyses were performed using custom software written in Matlab (Mathworks, Natick, MA). Only days that contain data from at least two animals were included, and all analyses excluded times when animals were moving along the track at a

speed below 3 cm/s to ensure that periods of non-spatial firing during immobility did not contribute to our results. The average activity for each cell was calculated as the total number of spikes for the run session divided by the session length (~15 minutes). When comparing cell rates across days, only the first run session was used from each track per day. To measure place field properties we calculated the 'linearized' activity of each cell (Fig. 1c). The behavioral data were separated into four trajectories (center arm to left arm, left to center, center to right, and right to center) and the animal's linear position was measured as the distance in cm along the track from the reward site on the center arm. We then produced four corresponding occupancy maps and spikes per bin maps using 2 cm spatial bins. Both the occupancy and spikes per bin map were smoothed with a 4 cm standard deviation Gaussian curve with a total extent of 20 cm. The spikes per bin map was divided bin by bin by the occupancy map to produce a smoothed, occupancy normalized firing rate map. Spatial peak rate was defined as the maximum rate across all spatial bins for one 15 minute run session. We excluded times when the animals were moving less than 3 cm/sec from all analyses. This removed periods of inactivity where spatial firing is less prevalent, ensuring that the place field shapes could be compared across animals and recording sessions. The similarity of spatial coding for single cells across the two environments was computed using place field overlap, defined as two times the sum of the overlapping areas of the linear rate curves divided by the sum of the areas of each curve [45]. This measure is bounded between 0 and 1, where 1 signifies perfect overlap. All trajectories with at least 3 Hz peak rate were averaged together for this measure.

We then examined the relationship between the spatial peak rate and the proportion of the environment over which each neuron was active. The proportion of the environment over which each neuron was active was defined as the set of places where the cell fired at above 0.5 Hz linearized firing rate. To do so we chose, for each neuron, the first session on the most novel track on each recording data. This restricted the analyses so that the same cell did not provide two data points for different blocks. The results were indistinguishable if this condition was relaxed (not shown). All statistical tests for differences in proportions used the Z-test for proportions, and the associated Z scores are reported in the text.

To characterize the changes we saw in spatial peak rates over time we constructed smoothed probability distribution functions (PDF) of peak and average rates. To do so we computed the cumulative distribution function (CDF) of the data, smoothed the CDF using a gaussian and computed the PDF as the derivative of the CDF. The guassian had a standard deviation of 2.3 Hz for the peak rate analysis and a standard deviation of 0.23 Hz for the average rate analysis. The width of the gaussian was ten times the standard deviation. Note that these smoothed distributions were used only for visualization and all statistics were computed on raw data.

We also developed a simulation approach to determine whether a measured set of within day changes in peak spatial rate seen between days 3 and 6 (referred to as the middle block) could account for the changes we observed from the first two days (early block) to the final days (days 7 onward, late block). To do so we first constructed a scatter plot with the peak spatial rate of each middle block neuron on the x-axis and the change in that peak rate from the first run of the day to the second run of the day on a

track on the y-axis (Supplemental Fig. 2). We then took individual cells from the early block, chosen at random, and simulated the evolution of their peak firing rates using the raw peak rate / change in peak rate data from the middle block. For each early block cell we computed its peak spatial firing rate and then found the middle block cell whose peak spatial firing rate during the was closest to that of the early block cell. We then took the change in the peak rate for the selected middle block cell and applied that change to the peak rate of the early block cell. Thus, a new peak rate for the early block cell was obtained by either increasing or decreasing the cell's peak rate according to the rate change of the matched cell from the middle block. This allowed us to apply the changes in peak rate we measured within a day for the middle block to the early block, thereby evolving the early block population according to the dynamics of the middle block cells.

We repeated the same procedure for the next iteration using the newly generated rate for the early block cell as illustrated in Supplemental Fig. 2. Peak rate changes from the middle novelty block were randomly sampled with replacement to match the size of the actual pool of cells. This meant that single cells could be picked multiple times from the early novelty block without duplicating a particular set of changes in rate. During the evolution process, any cells that dipped below 0 Hz peak rate were set to 0 Hz before the next iteration. The evolution process was repeated with 10,000 random cell picks from the early novelty block, each with 100 iterations through the process.

We also calculated the distributions that would result from random peak rate vs. peak rate change relationships. We chose at random a measured peak rate for each neuron and, separately, a measured peak rate change. We then used that population to simulate the dynamics of the early block group. This process was repeated 200 times.

These simulations occasionally produced 'runaway' cells whose rates went above 70 Hz, and we excluded these cells from the final distribution. Runaway cells did not result from the simulation based on the actual peak rate - rate change distribution.

Finally, we examined sharp-wave ripple (SWR) events during the rest following the first run of each day to determine whether the changes in rates that we found persisted after the initial experience in the environment into periods that have been associated with memory consolidation [43, 44, 46]. SWRs were identified based on peaks in the local field potential (LFP), recorded from one channel from each tetrode in the CA3 and CA1 cell layers. A reference tetrode was positioned the corpus callosum and all neural signals were recorded relative to that reference to eliminate muscle artifacts from the recordings. The raw LFP data were band-pass filtered between 150-250 Hz and the SWR envelope envelope was determined using a Hilbert transform. The envelope was smoothed with a Gaussian with a standard deviation of 4 ms and a width of 32 ms. SWRs were identified as times the smoothed SWR envelope stayed above 3 standard deviations of the mean for at least 15 ms on at least one tetrode. The full SWR events included times immediately before and after the triggering event during which the envelope exceeded the mean.

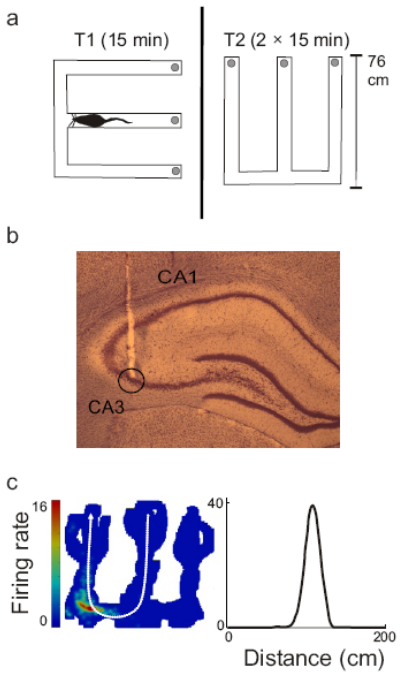


Figure 1. Experimental overview. a. Track shapes and orientations in the recording room. The track arms were 76 cm long and each section of track was 7 cm wide. The gray circles at the end of each arm represent food wells where rewards were delivered. The black line separating the two W-tracks represents the black barrier that prevented the animal from seeing one track from the other. The cartoon of a rat represents the approximate size of an animal relative to the environment. b. Histology. The slice shown contains a lesion from a tetrode targeting CA3. c. Linearization of firing rates. On the left is a 2-dimensional heat map of the occupancy normalized firing rates of one neuron. The animal's location was projected onto one of four linear trajectories. Shown on the right is the linear firing rate for one trajectory (shown in white on the heat map). The neuron had a peak spatial rate of 39 Hz and was active on 15% of the track. The linearized rate is higher than the non-linearized rate because the cell was highly directional and because two-dimensional smoothing reduces the firing rates.

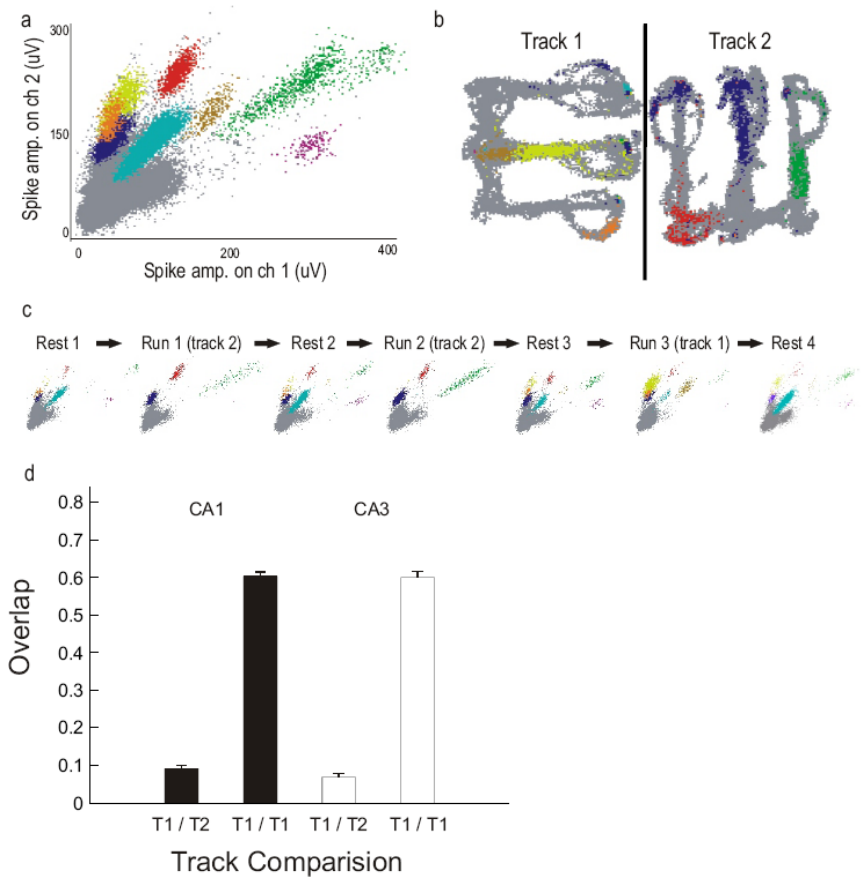


Figure 2. Distinct spatial representations for the two tracks. a. Spike amplitudes on two of four tetrode channels recorded during one recording session (experimental day 12, animal 6, group 2). Different colors represent different clustered cells; grey points represent spikes that were not clustered. b. Spiking as a function of position for a single run session on each track where each pixel in which a spike was detected is colored as in (a). The black line represents the barrier between the tracks. The differences in the spiking patterns between track 1 and track 2 illustrate the distinct spatial codes for these two environments. c. Example spike amplitude plots for each epoch illustrate the sequence of recording sessions, the stability of neural recordings across time and the differences in the set of activated cells across tracks. d. Overlap between the linearized

firing rates of the two runs from the same day across Track 1 and Track 2 (T1/T2) and two runs from the same day in Track 1 (T1/T1). The low overlap of T1 and T2 indicates that the spatial firing patterns of individual CA1 and CA3 neurons differed across these two environments, while the high overlap of T1 with itself indicates that the spatial representation of the first track was generally stable within a day.

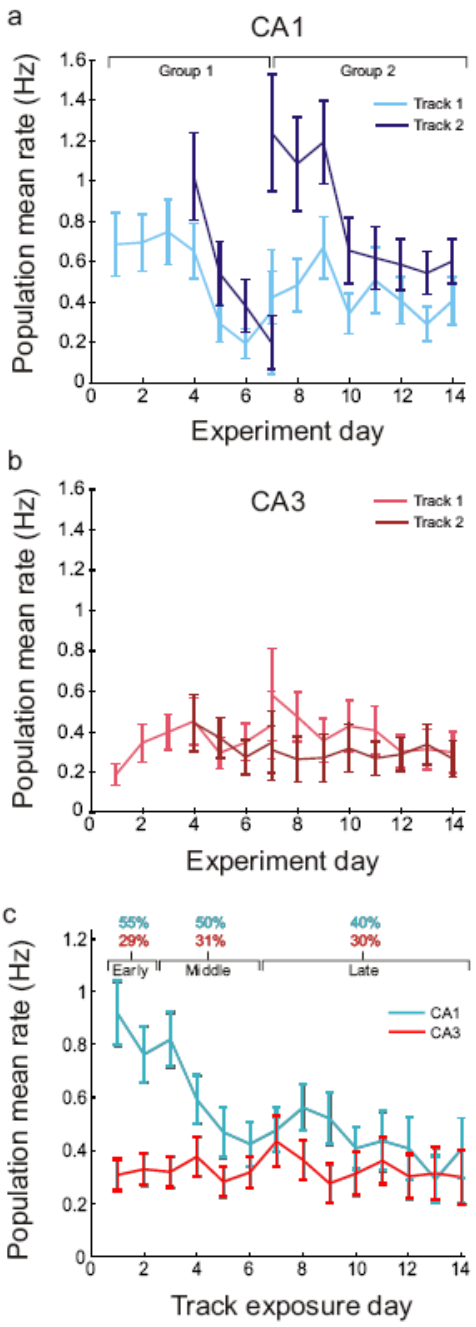


Figure 3. Hippocampal rate dynamics. a. Population average rates in CA1 as a function of experiment day. The set of days associated with each group is indicated at the top. Rates were high in each novel environment and then decayed over the course of a few days. Track 1, Group 2 illustrates the final firing rate level reached when animals had six days of experience on the track before recording began. b. Population average rates in CA3 as a function of experiment day. There were no significant changes in CA3 rates across days. c. Rates pooled from all animals and both tracks, plotted as a function of the number of days spent on the track. Top: percent of CA1 and CA3 cells active for the three novelty blocks, where 'active' is defined as having a mean rate > 0.1 Hz. Error bars represent SEM, calculated by repeated re-sampling of the data with replacement (bootstrap).

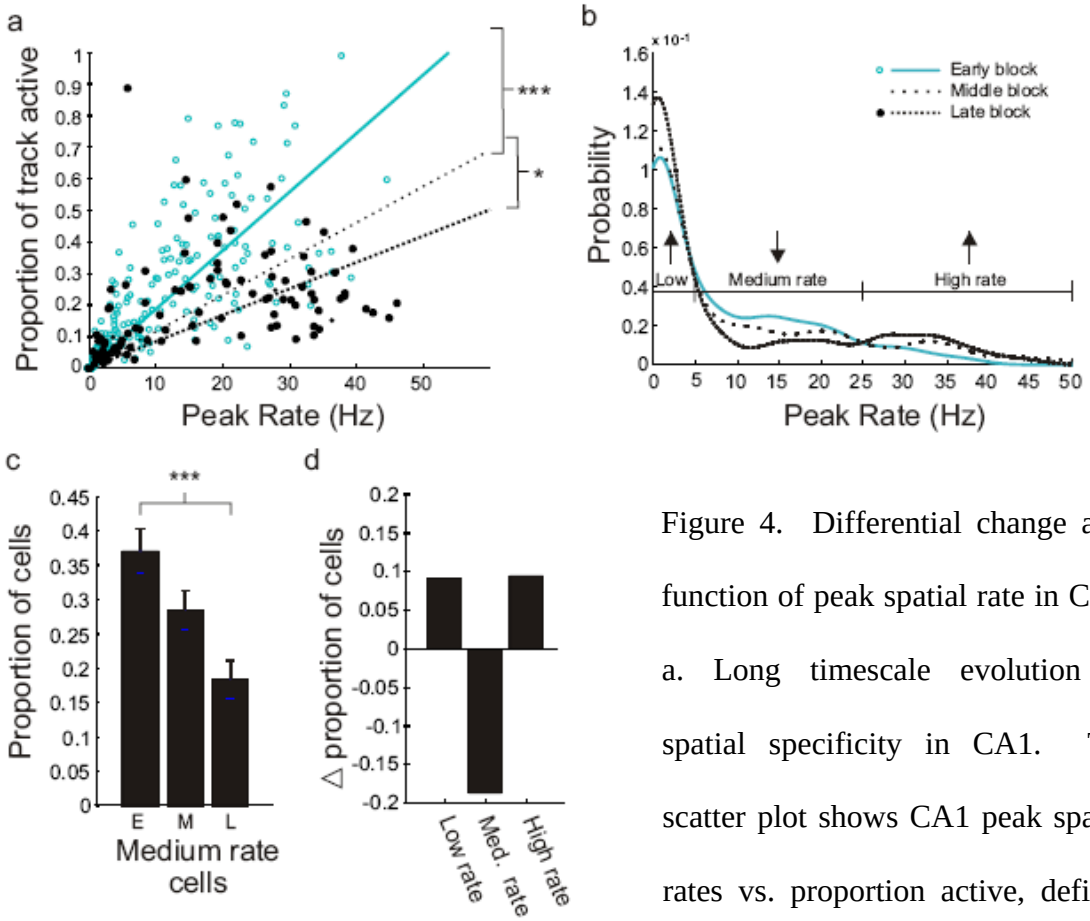


Figure 4. Differential change as a function of peak spatial rate in CA1. a. Long timescale evolution of spatial specificity in CA1. The scatter plot shows CA1 peak spatial rates vs. proportion active, defined as the proportion of the track where the cell had greater than 0.5 Hz linearized occupancy-normalized rate. Regression lines were constrained with a zero y-intercept. Points from middle block were omitted for clarity. There was a clear increase in specificity illustrated by the decrease in the slope of the regression line: high rate cells from the late block tended to cover smaller portions of the environment than high rate cells from the early block. b. Peak rate distributions for the early, middle and late novelty blocks. The distributions were smoothed for visual clarity, which reduces the sharp increase in proportion near zero, but all statistics were performed on the raw, unsmoothed data. The distributions were significantly different: early vs. middle, KS test, $p < 0.05$; early vs. late, $p < 0.001$. c. Proportion of cells in the intermediate 5 – 25 Hz peak rate groups as a function of novelty. There was a highly

significant decrease in the number of medium rate cells. d. Change in proportions for the low, intermediate and high peak spatial rate groups. The decrease in the intermediate group resulting in equal magnitude increases in the low and high groups. *, **, and *** represent $p < 0.05$, 0.01, and 0.001, respectively.

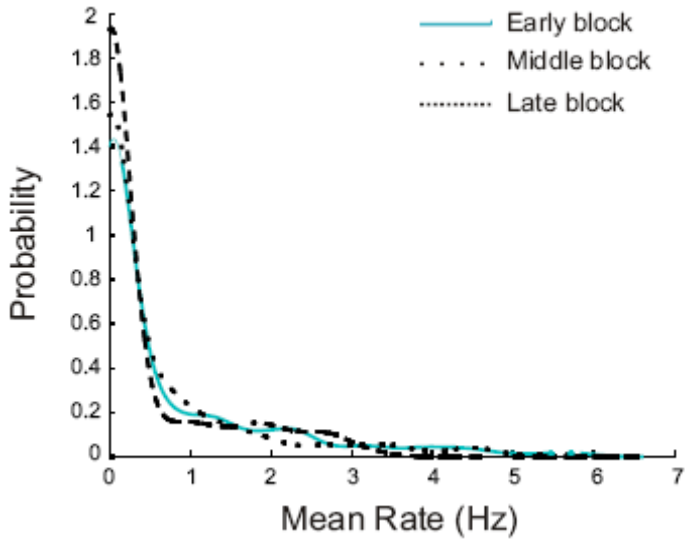


Figure 5. Cell selection process is not dependent on average rates. Shown are the mean rate distributions for the early, middle and late novelty blocks. While the average rate distributions did change somewhat, there was no evidence for selection based on average rate. Thus, our data indicate that the population selection rule did not depend on overall activity but was instead related to spatial specificity.

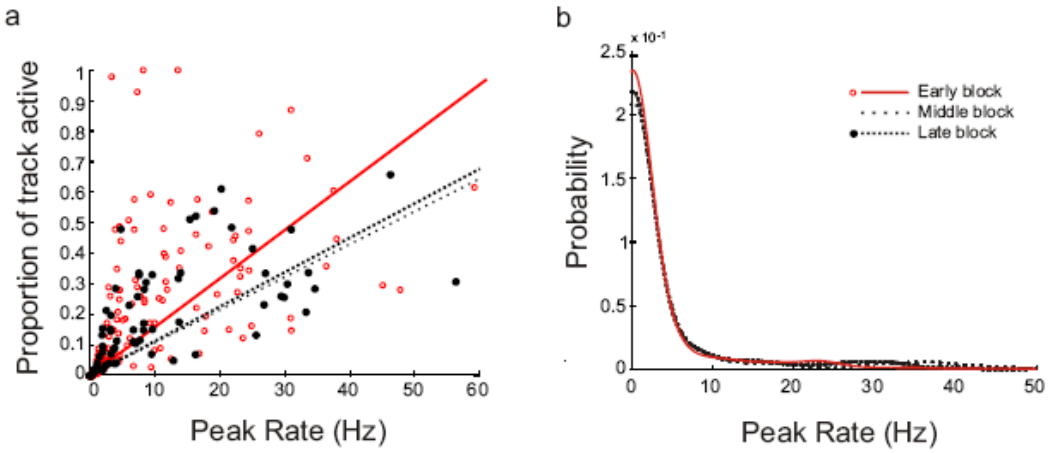


Figure 6. Smaller changes in spatial firing in CA3. a. Peak spatial rates versus proportion of the track on which each neuron was activity. Regression lines were constrained with a zero y-intercept. Points from middle block were omitted for clarity. There was a significant increase in specificity from the early to the middle block as illustrated by the decrease in the slope of the regression line ($p < 0.01$) but not subsequent decrease from the middle to the late block. Overall, cells remained active across large fractions of the track in both the early and the late blocks and there was no obvious increase in the number of high peak rate neurons. b. Peak rate distributions for the early, middle and late novelty blocks. The peak rate distributions of CA3 neurons changed only slightly, with a decrease in the proportion of peaks near zero and a slight increase in the proportion of high rate cells (KS test, early vs. middle, N.S, early vs. late, $p < 0.05$).

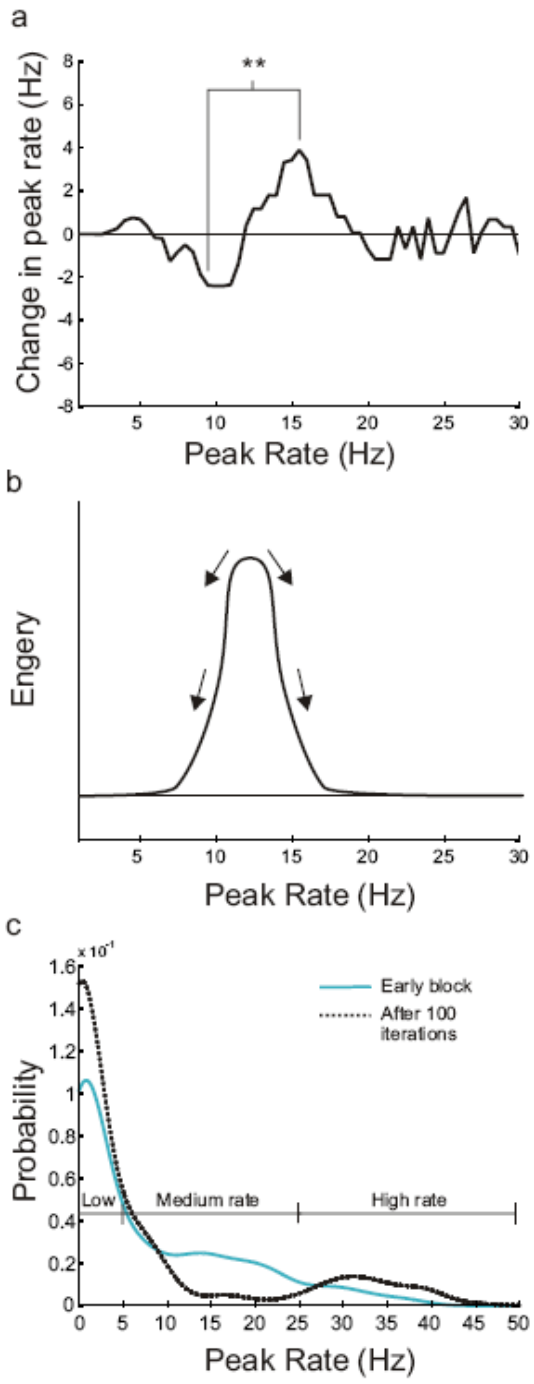


Figure 7. Within-day dynamics predict across day evolution. a. Peak rate vs. median change in peak rate from the first run to the second run in one day. Each point represents the median rate change for all data points in a 5 Hz sliding window along the peak rate axis. There was a clear and significant transitional from decreasing to increasing peak spatial rates for neurons with peak spatial rates between about 6 and 18 Hz. b. A cartoon of the associated energy surface, illustrating the dynamics expected from the measured peak rate changes. c. Peak rate distributions for the early novelty block and the 100th iteration of the rate dynamics simulation. The final distribution is similar to the distribution of the late block data. ** represents $p < 0.01$.

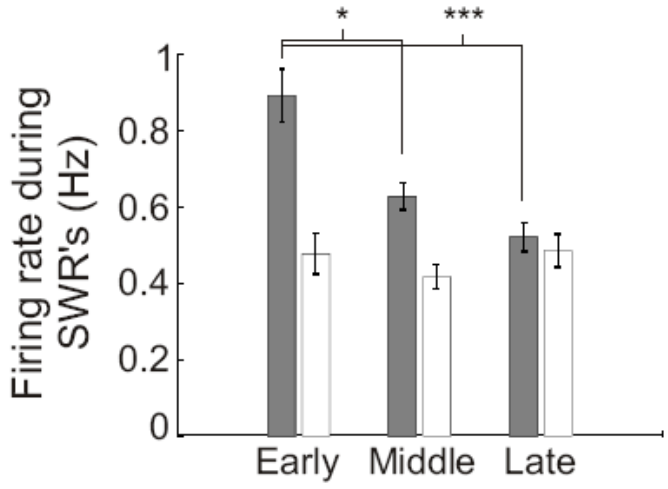
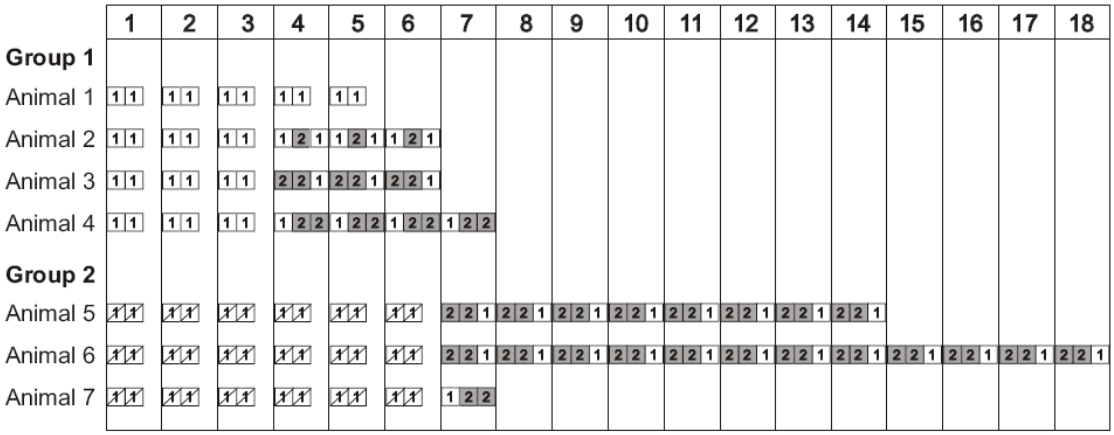
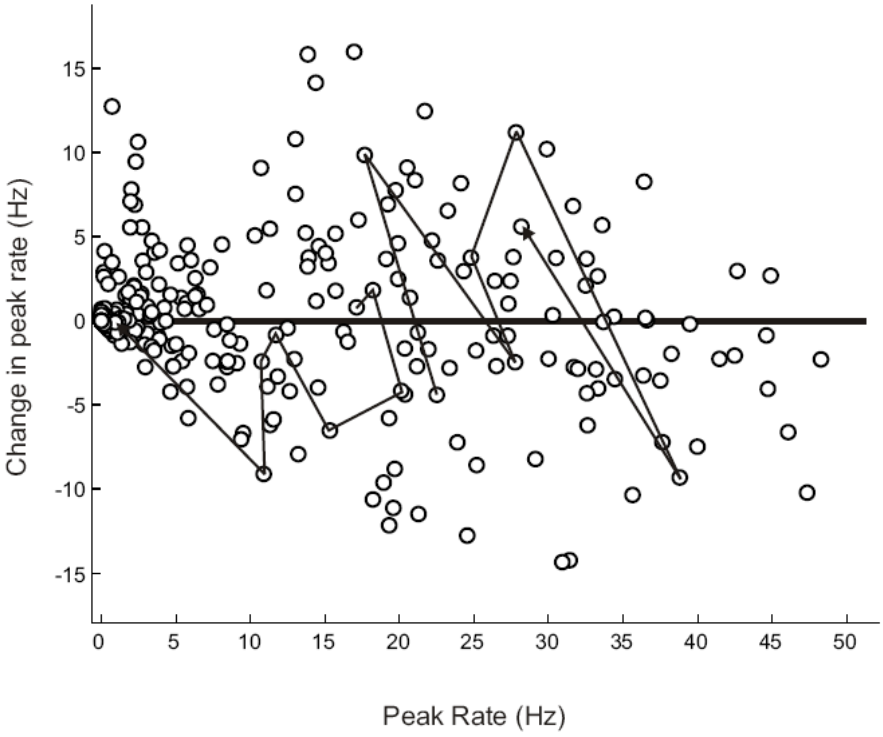


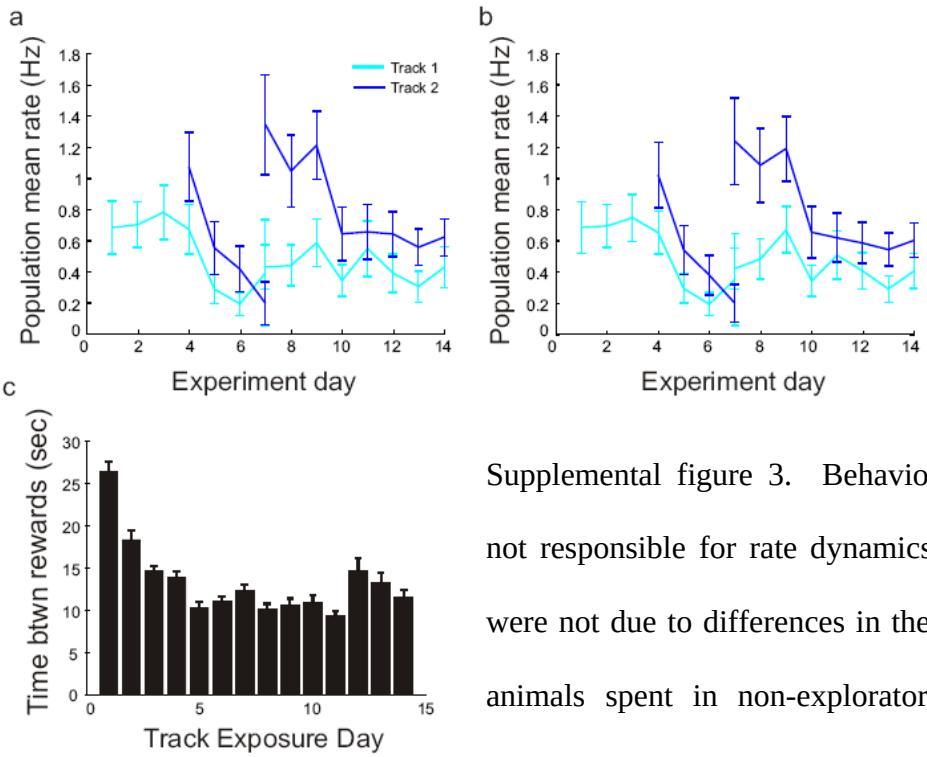
Figure 8. Firing rates during SWRs in the rest box following the first experience of each day. We detected SWRs and computed the firing rates of all recorded principle neurons from CA1 (grey bars) and CA3 (white bars). CA1 firing rates during SWRs declined rates across the three novelty blocks. In sharp contrast, CA3 SWR rates showed no such decline. These results are consistent with the idea that CA3 is involved in the initial memory formation process while CA1 remains plastic for longer times, and that CA1 activity changes throughout the time period associated with memory consolidation. * represents $p < 0.02$, *** represents $p < 10^{-4}$.



Supplemental figure 1. Recording schedule for each animal, organized for experiment day. White squares indicate a 15 minute run on track 1. Gray squares represent track 2. Squares with a diagonal line represent days when neural data were not collected.

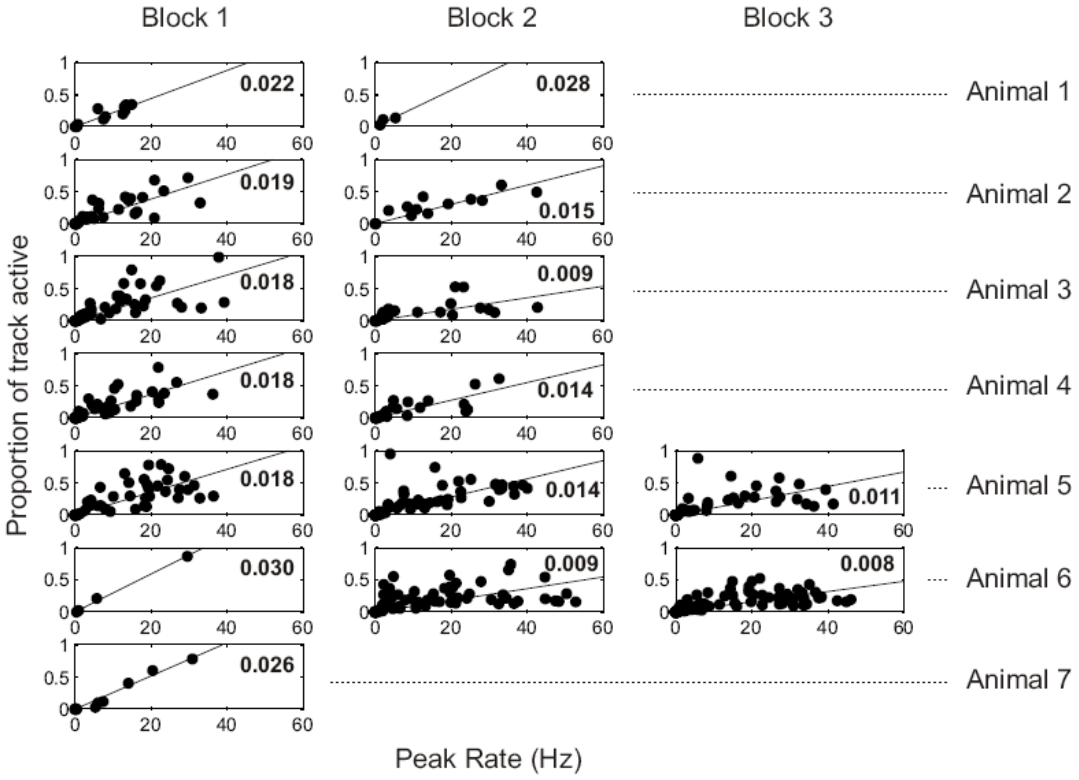


Supplemental figure 2. Demonstration of the simulation algorithm. Shown is the raw peak rate vs. rate change data from the middle novelty block, with two example 'walks'. One initial cell is picked at random from the early novelty block, and the cell from the middle novelty block whose peak spatial rate was closest to that of the early block cell is chosen. A new peak rate for the early block cell is obtained by either increasing or decreasing the cell's peak rate according to the rate change of the matched cell from the middle block. The same procedure is then repeated with the new peak rate of the early block cell, and so on. The result is that each early block cell evolves repeatedly according to the changes seen within a day during middle block.

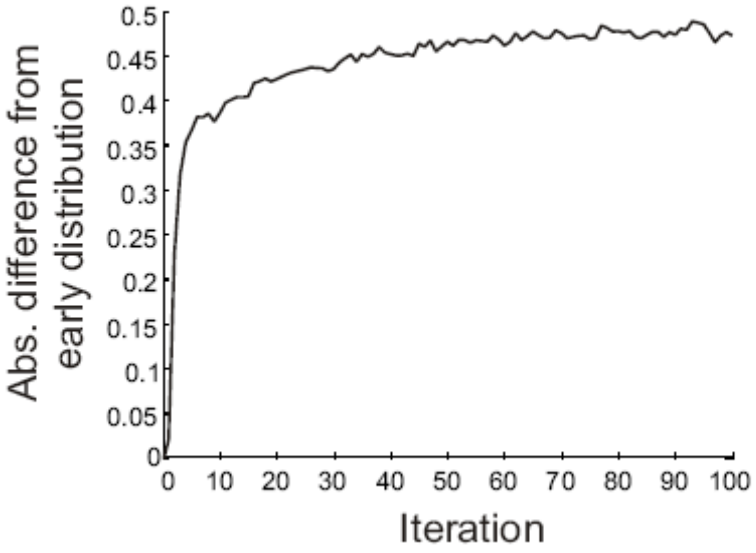


Supplemental figure 3. Behavioral factors were not responsible for rate dynamics. Rate changes were not due to differences in the amount of time animals spent in non-exploratory states, as all analyses excluded times when animals were moving along the track at a speed below 3 cm/s. The lack of rate change in CA3 implies that only behavioral modulations specific to CA1 could have contributed to our results, and to ensure that this was not the case, we recalculated the population mean rate while excluding different forms of behavioral variability. a. Differences in rate persisted when we excluded periods when animals were turning around in the environment or hanging over the side of the track. Shown are the mean CA1 population rates, excluding all data from when animals turned their heads more than 15 degrees off the direction of the track along with all times when the animals' linear speed dipped below 3 cm/sec. b. Rate trends remained after excluding activity that co-occurred with ripple events in the local field potential, which have recently been shown to increase in frequency during novel experiences [47]. Ripples times were detected using a very liberal algorithm defining a ripple as any period during which the envelope of the 150 – 250 Hz filtered LFP trace

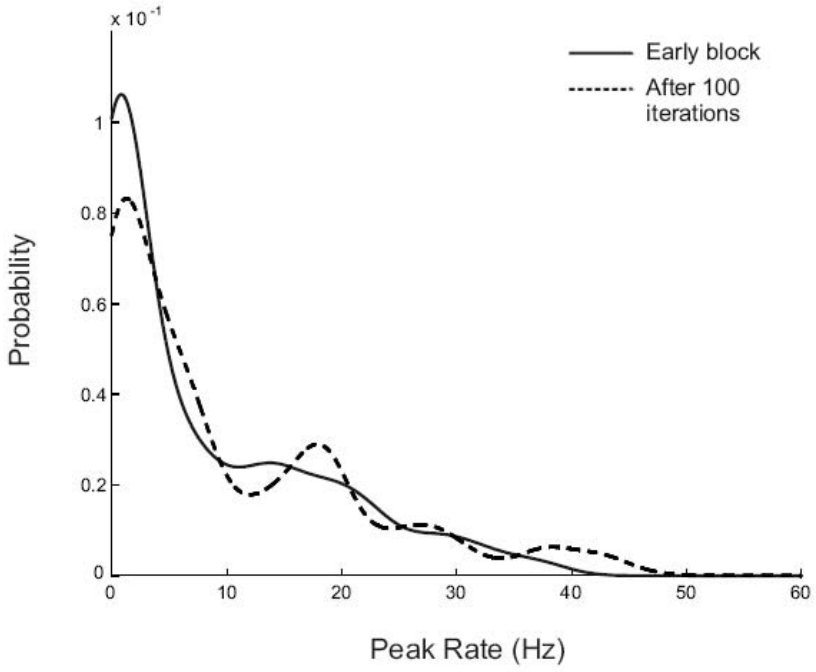
from any of the tetrodes exceeded two standard deviations from its mean. This included many smaller amplitude events that might normally be excluded from ripple analyses, and the exclusion of all of these events renders our ripple analysis highly conservative. c. Time between arrivals at consecutive reward locations as a function of track exposure day. Animals generally moved more slowly in the novel track, and thus the higher rates seen in novel environments were associated with lower movement speeds. This is exactly the opposite of what we would expect given the previously established positive correlation between speed and CA1 firing rates [33], and strongly suggests that movement speed modulation cannot account for observed differences. Error bars represent standard deviations, calculated by repeated re-sampling of the data with replacement (bootstrap).



Supplemental figure 4. Peak rate vs. proportion of track active for CA1, separated by animal and novelty block. For each plot, the slope of the regression is shown in bold. Except for animal 1, from which relatively few CA1 cells were recorded, the slopes always decrease from blocks 1 to 2 and from blocks 2 to 3, indicating consistent place field dynamics across animals.



Supplemental figure 5. Convergence of simulated early block cells using middle block dynamics. The Y axis represents the absolute difference in area between the original early block rate distribution and the simulated distribution. The simulated distribution becomes stable after about 100 iterations. It is not clear that the number of iterations can be directly mapped to a length of time for the animal, as the precise rate of change is likely to be due to complex interactions between the number of run sessions and the amount of sleep the animal experience between them. Nonetheless, after 100 iterations the resulting distribution was similar to the final late block distribution from the late block (days 7 – 11) of the actual data.



Supplemental figure 6. Example of a simulation with scrambled peak rate–rate change relationship. We matched the peak rates from cells in the middle novelty block with a scrambled set of the rate changes, and performed the simulation. Shown are the rate distributions from the early block, and one simulated distribution using the scrambled data. We repeated this procedure 200 times, and did not observe a single instance where the changes we saw were within the distribution of changes produced by the simulation, indicating that these changes are highly unlikely to be due to chance ($p < 0.005$).

Chapter 2

Spatially and temporally remote replay of hippocampal memories during waking behavior

Introduction

Hippocampal "sharp wave" events are believed to be important for memory consolidation[44, 48-50]. These events are associated with oscillatory bursts of network activity that generally originate in CA3 and propagate through CA1 and adjacent cortical regions[43, 51], and are thought to allow recently formed hippocampal memories to be transferred to slower-learning cortical areas. Recent studies have observed that during sleep and quiet immobility immediately following exploration of an environment, sharp waves tend to activate similar patterns of activity as seen during the preceding experience. Hippocampal place cells that fired together during exploration become more likely to fire together during sleep[46, 49, 52-54] where the sequence of visited place fields can be replayed at high speeds[55-58]. These results demonstrate that patterns of activity corresponding to an experience are stored and then reactivated following that experience. Further, in combination with behavioral studies of learning in relation to sleep[59-61], these findings provide strong evidence that sleep plays an important role in off-line processing of new memories.

But does memory reactivation also occur during wakefulness? Recent studies have observed sequence replay occurring during awake exploration[28, 62, 63], suggesting that activity relating to consolidation may also occur during awake states[28]. The reported awake-activated sequences always replayed the environment the animal was currently in,

however, and they initiated at the animal's current location in that environment. This observation has been taken to indicate that awake replay results from sequential activation of otherwise subthreshold place fields[28, 62, 63]. This model suggests that awake replay is different than sleep replay, in that awake replay depends on current sensory input while sleep replay is a reactivation of a stored memory.

If, on the other hand, waking and sleep replay are fundamentally similar phenomena that both involve the recall of memories, we would expect that animals could replay experiences of one place while awake in a different place. We therefore examined replay of sequences of hippocampal place cells from the CA3 and CA1 regions of the hippocampus to determine whether memory retrieval was important for both waking and sleep replay. We exposed animals to multiple environments presented sequentially. We then established the spatial mapping of one environment from a recorded set of place cells in the hippocampus and asked whether replay during subsequent awake experiences in a different environment was consistent with the neural representation of the first environment. We found clear evidence for long lasting replay of hippocampal memories consistent with a role for awake replay as an element of memory retrieval and consolidation.

Results

Track 2 (T2) had a W-shaped geometry, with one reward site at the endpoint of each arm (Fig. 1a,b), and animals were rewarded for performing a continuous alternation task (center-left-center-right-center, and so on). During run sessions in T2, we simultaneously recorded groups of putative pyramidal neurons in both CA3 and CA1,

many of which showed spatially selective activity. As expected, the cells fired in sequence as the animal moved through the environment (Fig. 2a). Subsequent awake recordings of the same cells were taken both during a non-rewarded rest period in a high-walled box and during a run session in a second environment (T1). Animals were placed in the rest box for 20 minutes before and after each run session, and each recording day consisted of two run sessions in T2 followed by a single session in T1 (Fig. 1b). T2 was always more familiar than T1, and animals had between 3 and 12 days of experience in T1 and between 4 and 18 days of experience in T2. The pattern of exposures across days and animals is shown in Supplemental Fig. 1. To avoid confusing replay events and sequential firing during phase precession, we restricted our analyses to sharp waves ripple events (SWRs) that occurred when animals were moving less than 2 cm/sec.

We found that awake replay of T2 continued after animals were removed from T2 and placed in the rest box. Activity from the two rest box sessions that followed an exposure to T2 was similar, so we combined data from the two rest sessions. To be conservative, awake periods were defined as times when animals had been immobile no more than five seconds, which on average represented approximately half of the rest session time. These awake SWRs are similar to events previously referred to as eSWRs[64] (exploratory SWRs). In sharp waves occurring during these periods we observed clear replay of T2 place fields in a spatially consistent order (Fig 2b-e). These events immediately preceded or followed periods of movement, sometimes across the entire box (e.g. Fig 2c, e), and thus corresponded to times when the animal was awake.

Using an established approach for visualizing replay events[28, 62, 63], we ordered place cells by the distance of each cell's place field peak from the endpoint of the center

arm of T2. Replay events can only be detected if a sufficient number of cells with place fields are activated, and we therefore defined candidate replay events as sharp waves activating 5 or more cells with place fields in T2. Individual replay events are then visible as diagonal sweeps of five or more spike trains, where sweeps traversing away from the center arm are upward sweeps and those traversing towards the center arm are downward sweeps. In rare occasions the sweeps went from one outer arm to the other, in which case the cells were ordered as a function of the distance from the end of one of the outer arms. To test the significance of each replay event we used a simple Bayesian decoder with an uninformative prior to translate the spike sequences into positions in T2. Each SWR event was divided into 15ms bins, where each bin represented one decoding time step. The output of the decoding algorithm provides a probability distribution across all locations in T2 for each time step (Fig 2c,e). These probability distributions allowed us to perform a regression analysis on each sweep (see methods). To test the probability of a sweep occurring by chance we compared the regression R^2 value to the R^2 values obtained after scrambling the time bins (10,000 comparison permutations for each event). Sweeps that were unlikely to occur by chance at the $p < 0.05$ level were considered to show replay, as these sweeps represented coherent sequential activation of spatial representations.

We found that 256 out of 580 (44.1%) of candidate events showed significant replay of T2 during awake periods in the box, which is many more than the 5% expected by chance ($Z = 15.48$, $p < 10^{-10}$). These awake replay events occurred consistently across all three animals (animal 1, 5/22 events; animal 2, 149/346 events; animal 3, 102/212 events; all p's < .05). The proportion of significant events was very similar to the

proportion computed for run sessions in T2 (Fig. 2b; 288 out of 612 events significant, 47.1%; rest vs. T2: $Z = 1.01$, N.S.), demonstrating that awake replay of previously experienced and spatially distinct environments is as prominent as replay of the currently experienced environment. We should note that these replay events occurred in both directions of the track, but as the majority of the place cells we recorded were active in both directions of motion, these replay events could not be meaningfully classified as either forward or reverse events[62, 63].

We then compared the prevalence of replay during these waking episodes with replay during periods of quiescence in the rest box where the animal was immobile for longer periods of time. The commonly accepted idea that consolidation occurs primarily during sleep predicts that replay activity would be most robust during quiescence, but we found that this was not the case. We first defined periods of quiescence as times when animals had been immobile for five seconds or longer. Many events occurred after minutes of immobility (Supplemental Fig. 2a), likely signifying sleep, but this threshold likely included a number of awake periods, and is therefore less likely to reveal differences between waking and quiescent replay than by using a higher immobility threshold. To our surprise, however, we found that replay of T2 during these SWRs was less likely to occur: 373 out of 1046 (35.7%) of candidate events showed significant replay (awake > quiescence, $Z = 3.36$, $p < 0.001$; Fig. 3a). Using a more stringent criterion for quiescence (immobility for more than 60 seconds), we found that once again the proportion of replay events was lower in quiescence as compared to awake periods (106 out of 310 events, 34.2%, $Z = 2.88$, $p < 0.005$).

The observed difference was not due to a lack of activity from T2 place cells during quiescence, as firing rates for individual T2 place cells during quiescence were on average higher than the rates of those same cells during waking. We compared individual neuron's firing rates during SWRs in the awake and quiescent periods and found that, for the large majority of cells (217 out of 244), rates were higher during quiescent periods ($Z = 9.34$, $p < 10^{-10}$; Fig. 3b). This was consistent with the greater number of candidate replay events with five or more place cells activated during quiescence (1046 vs. 612 during awake). Given that a candidate event occurred, however, it tended to activate fewer place cells in the quiescent than in the awake state (ranksum, $Z = 6.65$, $p < 10^{-10}$; Fig. 3c) and in particular candidate quiescent events were more likely to activate 6 or fewer cells while candidate awake events were more likely to activate 7 or more cells. Thus, while overall SWR spiking is decreased during the awake state, population activation tends to be more concentrated in select SWRs. This increased coherence may facilitate more precise replay when animals are awake.

While the comparison of the number of replay events for the same population of place cells is meaningful, the absolute number of replay events detected on one day will depend on the total number of neurons with place fields recorded. As an example, if only five neurons with place fields were recorded on a given day, the number of candidate events (e.g. events where all five active cells were firing) would be relatively small, but as the number of cells with place fields goes up, the number of candidate events increases. We therefore developed a complementary analysis approach that is much less sensitive to these sampling issues. We computed the cross-correlation of spike trains from all pair-wise combinations of simultaneously recorded place cells and plotted the

histograms as a function of the linear distance between the place field peaks (see methods). For display purposes each histogram was normalized so that the peak was displayed in red and the trough in blue (Fig. 3d). During both wakefulness and quiescence we observed an average spike latency of 0 ms for cells with co-localized place fields in T2. This latency widened with longer distances between place fields, showing that place cells are activated in precise temporal order. Cross-correlation latency was often observed as two peaks offset from zero, instead of one, showing a bi-directional replay relationship for many cell pairs. Thus, with all cross-correlations stacked as a function of distance between fields, population replay is observed as an expanding 'V' centered at 0 ms latency. We calculated how well the distances between place fields explained the observed spike latencies using a linear regression between place field distance and relative spike timing applied to the raw, non-normalized data (see methods), and observed a stronger linear relationship during wakefulness than during quiescence (awake $R^2 = 0.1248$ with 45228 spike pairs; quiescent $R^2 = 0.0715$ with 40074 spike pairs, awake > quiescent $Z = 13.87$, $p < 10^{-10}$; Fig. 3e). Thus, replay activity was less precise during quiescence when we analyzed all spikes occurring during SWRs, a result consistent with our findings for replay events.

The clear presence of awake replay in the rest box suggests that the hippocampus might be able to activate representations of multiple environments in close succession by switching between the currently experienced environment and recently explored environments. To explore this, we examined activity in SWRs during run sessions in the second environment (T1). Unlike the rest box, where few neurons had place fields, T1 was large enough to allow replay sweeps. T2 and T1 had identical w-shaped geometries,

and animals were rewarded for performing the same alternation task in T2 (Fig. 1). The population mapping of place fields in the two environments was always very different, indicating that the animals formed a distinct spatial representation of each environment (Supplemental Fig. 3).

Animals were generally highly motivated to obtain rewards and were immobile for only relatively short times during the 15 minute sessions (Supplemental Fig. 2b). Because the animals were always awake, we did not confine our definition of awake sharp waves to immobility periods of less than 5 seconds, as this definition was mainly used during rest sessions to be conservative about the definition of wakefulness. When animals were located in T1, 182 out of 442 (41.2%) candidate replay events showed significant replay of T2, which is many more than expected by chance ($Z = 12.67$, $p < 10^{-10}$; Fig 4a). At the same time, 147 out of 330 (44.6%) candidate T1 replay events showed significant sweeps of T1. These proportions were similar if we used a 5 second immobility cutoff to exclude longer periods of immobility (96/227 for T2 replay- 42.3%, and 90/190 for T1 replay- 47.4%) or even a 2.5 second cutoff (53/123 for T2 replay- 43.1%, and 48/105 for T1 replay- 45.7%). Out of the 182 replay events for T2, 24 (13.2%) showed simultaneous replay of T1. Out of all significant replay events for T2 and T1 (182 for T2 + 147 for T1 - 24 simultaneous T2 and T1 events), over half (182/305; 59.7%) were significant replays of T2, showing that replay of previously visited environments makes up a large proportion of awake events. This may have partially been due to the fact that T2 was always relatively more novel than T1 (see methods), increasing its probability of being replayed[47].

Because T2 and T1 had identical geometry, one could imagine that the animals confused T1 for T2, causing replay activity that was not truly remote. This is unlikely, however, as we found that the large majority of T2 replay events did not coincide with detectable replay of T1 (158 T2 only replay events out of 182 total T2 replay events). Thus, replay differentiated between the two tracks. Furthermore, if the replay events were due to a confusion of the two tracks, one might expect that replay of T2 would initiate at the animal's corresponding location in T1, similar to what was previously observed for non-remote awake replay. To address this possibility, we reasoned that at times when an animal is located at one of the three endpoints of the W-track, sweeps must travel in the direction extending away from that endpoint if they are initiated at the animal's location. This was not the case, however, as the sweeps moved away from the animal's location only about half the time (85 out of 158 events, 53.8%, $Z = 0.68$, N.S.). Thus, nearly half of the events were decoded as moving towards the corresponding position of the animal in T2, showing that replay of T2 was effectively decoupled from the animal's current location in T1. Furthermore, for the 24 events where both tracks were replayed simultaneously, the direction of the pairs of T2/T1 replay events was not significantly correlated (Pearson's $R = 0.34$; N.S.). For comparison, replay events occurring during exploration of T2 were generally tied to the animal's position in the track (151 out of 190 events, 79.5%; more than half: $Z = 6.01$, $p < 10^{-8}$). We should note though, that the presence of the 20.5% of the events that were not tied to the animals' current position in T2 establishes that replay events of the environment the animal is presently experiencing are not exclusively bound to the animal's current location.

The pair-wise analysis confirmed the presence of replay of T2 while the animal was in T1, in that there was a clear relationship between place field distance and pair-wise spike timing (Fig. 4b). Here, we excluded cells that had place cells in both environments, as their contribution to both types of replay interfered with the analysis of each environment separately. Thus, T2 place cells that were largely inactive during exploration of T1 still showed clear, ordered replay activity during sharp waves. Interestingly, the pair-wise regression analysis for T2 cells while the animal was in T1 yielded a higher R^2 value than for awake periods in the rest box (regression R^2= 0.1736, compare to rest, $Z = 8.57$, $p < 10^{-10}$), suggesting that some aspect of the task facilitated more precise replay dynamics despite animals being awake in both cases.

Finally, animals were placed in the rest box one last time. Here, we observed significant replay of both environments in the awake state, with 51 out of 147 (34.7%) candidate T2 events being significant, and with 58 out of 128 (45.3%) candidate T1 events being significant. This result is consistent with previous analyses of pairs of neurons following exposure to multiple environments[53]. The decline in the proportion of T2 replay events as compared to the previous rest was significant ($Z = 2.07$, $p < 0.04$) and confirms previous reports that suggests that the strength of reactivation goes down the longer the time from the initial experience[49, 53]. For both types of replay, however, the probability of replay was once again significantly lower during quiescence (T2 replay: 87/389 (22.4%), $Z = 2.91$, $p < .01$; T1 replay: 105/303 (34.7%), $Z = 2.09$, $p < .05$).

The described experimental sequence was repeated across multiple days for each animal. Therefore, it is possible that exposures from previous days contributed to observed replay. To determine if this was the case, we analyzed replay dynamics before

the first daily exposure to T2. Using both the event-based analysis and the pair-wise analysis, we observed no evidence for replay activity for either environment during the first rest session of each day (Fig. 5). The pair-wise regression yielded a significantly lower R^2value than for all subsequent behavioral epochs (regression R^2 = .025; compared to quiescence in rest box, Z = 8.30; to awake periods in rest box, Z = 15.25; to runs in T1, Z = 19.13; all p's > 10^{-10}). This demonstrates that while replay activity persisted for over an hour after an experience, it decayed significantly across days.

All aforementioned analyses were performed on both CA3 and CA1 place cells. This was done to maximize the number of place fields used to decode replay events. However, as previous replay experiments studying replay only studied replay in CA1, it is not clear whether CA3 participates in these events. We examined CA3 activity and, as expected[12], found that a relatively small proportion of CA3 cells had a place field in a particular environment. As such, it was not possible to examine a sufficient number of candidate replay events from CA3 neurons alone. Nonetheless, using our pair-wise analysis we found evidence for robust replay activity in CA3 (Fig. 6). We also found that that the relationship between place field distance and spike timing between cell pairs was stronger during the awake SWRs in both CA3 and CA1 when these areas were analyzed individually (CA3: Z = 6.59, p < 10^{-10}; CA1: Z = 5.96, p < 10^{-8}), justifying our decision to combine cells from both areas in our main analyses.

Discussion

We observed spatial replay in three different behavioral conditions: 1) awake replay of the currently experienced environment, 2) awake replay of a remote

environment and 3) remote replay during extended periods of sleep-like quiescence. Awake replay events tend to initiate at the animal's current location if the animal is still located in the environment, but did not always do so, indicating that current sensory input is not always the dominant driver of local replay events. Further, when animals are placed elsewhere, robust awake replay continues in both in the rest box and during goal-directed behavior in a different environment. Surprisingly, we found that the precision of replay activity declined significantly when animals were quiescent in the rest box. Overall, our results indicate that replay events are a manifestation of the retrieval of previous experiences, and that this retrieval is of higher fidelity during states more closely associated with waking behavior.

These results indicate that current models of awake replay require modification. These models[28, 62, 63] posit that the activation order of neurons within an eSWR event stems from a sweep of increasing excitation interacting with subthreshold spatial inputs to those cells. The idea is that the region of space in which a place cell is active is akin to the tip of an iceberg, and that each cell receives subthreshold inputs from well outside the place field. These inputs would be expected to decrease in strength as a function of increasing distance to the place field center. A SWR event would be a sweep of increasing excitation, and thus neurons with place fields at the animal's location would fire first and neurons with place fields farther away would fire later, as their initially subthreshold membrane potentials would require more time to reach threshold.

This model implies that awake replay events should always originate at the animal's current location, but our data establish that this is not the case. About 20% of replay events in the first environment (T2) moved toward, rather than away from, the

animal, indicating that they originated with cells representing locations distant from the animal. Further, we saw replay of T2 during awake episodes in both the rest box and in the second environment (T1). It is difficult to reconcile these awake replay events with the subthreshold spatial input model for four reasons. First, the spatial representations of three environments were distinct, so the replays of T2 did not correspond to spatial sequences from the rest box or T1. Second, the replay of T2 was not related to the animal's spatial location in T1. Third, only about 5% of the T2 replay events were also significant replay events for T1, indicating that the spatial structure of T1 was seldom visible during these events. Finally, the pair-wise signature of replay of T2 was clearly present while the animal was in T1 even after we excluded all cells that had place fields in T1. Thus, while there is good reason to believe that subthreshold place fields could contribute to sequence replay for the environment the animal is currently experiencing[57], this model is not sufficient to explain our results.

Our data are instead consistent with a model where both waking and sleep replay depend on recall of stored memories representing sequences the animal has experienced in the past. Given that we saw clear evidence for structured replay in CA3, where SWRs generally originate[51], one possibility is that replay constitutes activation of a sequence stored in the CA3 associative connections. How then would a specific sequence become activated? We would expect that current inputs could bias the network to retrieve sequences associated the animal's current location, as is the case in the 80% of replay events of T2 when the animal was in T2. We would also expect that similarities between current inputs and inputs present in a remote environment could activate a "seed" group of neurons in one environment that lead to replay of remote environment, a possibility

consistent with our observation that replay of T2 was more precise in T1 than in the rest box. This would serve as a basis for associative recall. Furthermore, given results demonstrating increased reactivation of neurons associated with recent novel experiences[47, 65], we would also expect strong replay of a more novel experience in a more familiar environment, a result consistent with our observation that about 60% of the detectable replay events in T1 were replaying sequences from the more novel T2. We therefore suggest that these replay events are the hippocampal manifestation of memory recall. We should note, however, that whether the recalled memory trace leads to widespread reactivation of neocortical regions is likely to depend on the state of the neocortical networks, and thus hippocampal replay events are likely to be necessary, but not sufficient for full brain memory recall events.

The recall events we observed were present in both waking and more sleep-like states, but were of higher fidelity in the awake state when the animal had recently been in motion. Overall SWR firing rates were higher during quiescence, however, indicating that the less coherent replay was not due to global inhibition of the network. Instead, these results suggest that inputs that drive memory retrieval in the hippocampal network are less well organized during quiescence or, alternatively, that the hippocampal network itself is noisier during this state. In either case, our findings suggest that awake replay is, on average, better organized than sleep replay and could therefore play an important role in memory consolidation.

This came as a surprise to us given previous results that suggested either similar fidelity of waking and sleep SWR reactivation[53] or somewhat better reactivation in sleep as compared to waking[64]. These two reports examined activity from open field foraging

tasks, however, where it is not clear that spatial sequences are expressed in SWR events. We therefore suggest that the difference between our findings and previous results is due to the sequential nature of the animal's task, which should promote the formation of memories for specific sequences of places. In our opinion, this type of sequential task is more similar to human awake experience than random foraging, as events contain specific sequences of people, places and things.

Finally, we can ask whether the structure of these waking replay events would confer any particular advantages for memory consolidation. We found that the strength of replay declines over time, a result consistent with previous studies of pair-wise reactivation[49, 53], and we know that animals are not generally inclined to sleep immediately following each new experience. Thus, if consolidation were restricted to sleep, we would expect that experiences early in the day would be consolidated poorly if at all, while experiences closer to "bedtime" would be retained. The waking replay we found could provide a mechanism to ensure that all memories are replayed sufficiently often to allow consolidation into neocortical memory stores. Further, as a memory for a past experience can be replayed during a current experience, and as we occasionally saw significant replay of both environments at the same time, replay could facilitate the formation of associations that link multiple distinct experiences.

Methods

Data collection and pre-processing

Three male Long-Evans rats (500-600g) were food deprived to 85 – 90% of their baseline weight and pre-trained to run on a linear track with one reward site one each end of the track. This pre-training was performed in a different room from the recording experiments. After the animals were accustomed to behaving for liquid reward (sweetened condensed milk), they were implanted with a microdrive array containing 30 independently movable tetrodes (see Frank et al. [9] for details) according to UCSF and National Institutes of Health guidelines. The tetrodes were arranged bilaterally in two 15 tetrode groups centered at at AP -3.7 mm, ML ±3.7 mm. Each group was located inside oval cannula whose major axis was oriented at a 45 degree angle to the midline with the front of the cannula closer to the midline. Tetrodes in the anterior portion and lateral portion of each group targeted lateral CA3 while more posterior and medial tetrodes targeted CA1. After 5-6 days of recovery, animals were once again food deprived to 85% of their baseline weight. After 10 days of recovery, we began advancing the tetrodes toward the CA1 and CA3 cell layers over 2-3 days.

Animals were initially introduced introduced to W-track Track 1 (T1) either 3 (N = 1) or 6 (N = 2) days before being introduced to W-track Track 2 (T2), with two fifteen minute run sessions a day. Here we included only data from when animals were first introduced to T2 onward. From that point animals ran two sessions in T2, followed by one session in the more familiar T1. They were rewarded for performing a continuous alternation task where, starting from the center arm of the W-track, they alternated visits to each outer arm. Each outer arm visit was followed by a return to the center arm before

the next outbound trajectory was made. Errors were not rewarded, and following an incorrect choice of an outer arm no rewards were given until the animal returned to the center arm. This task took 3-6 days for animals to become proficient. Run sessions were flanked by 20 minute rest periods in a high walled black box. The floor of the box was 25 by 34 cm, and the walls were 50 cm tall. The W-tracks were 76 by 76 cm. Tetrode positions were adjusted after daily recording sessions for all tetrodes that had poor unit recordings. On rare occasions some tetrodes were moved before recording sessions, but never within four hours of recording.

Data were collected using the NSpike data acquisition system (L. Frank, J. MacArthur). The animal's position on the track was reconstructed using a semi-automated analysis of digital video of the experiment with custom-written software. After neural data was collected, individual units were identified by clustering spikes using peak amplitude and spike width as variables. Care was taken to only cluster well isolated neurons with spike waveform amplitudes that were clearly stable over the course of the entire session. All spike sorting was done using custom software (MatClust, M. Karlsson).

Analysis of neural data

All analyses were performed using custom software written in Matlab (Mathworks, Natick, MA). To measure place field locations we calculated the 'linearized' activity of each cell. The animal's linear position was measured as the distance in cm along the track from the reward site on the center arm. We then produced an occupancy map and a spikes per bin map using 2 cm spatial bins. Both the occupancy

and spikes per bin maps were smoothed with a 4 cm standard deviation Gaussian curve with a total extent of 20 cm. The spikes per bin map was then divided bin by bin by the occupancy map to produce a smoothed, occupancy normalized firing rate map. Place field peak rate was defined as the maximum rate across all spatial bins. The criterion for a cell being identified as a 'place cell' was having a place field peak rate of at least 3 Hz. Putative interneurons were identified based on spike width and average firing rate, and were excluded from all analyses.

Sharp waves ripple events (SWRs) were identified based on peaks in the local field potential (LFP), recorded from one channel from each tetrode in the CA3 and CA1 cell layers. A reference tetrode was positioned the corpus callosum and all neural signals were recorded relative to that reference to eliminate muscle artifacts from the recordings. The raw LFP data were band-pass filtered between 150-250 Hz and the SWR envelope envelope was determined using a Hilbert transform. The envelope was smoothed with a Gaussian with a standard deviation of 4 ms and a width of 32 ms. SWRs were identified as times when the animal's head velocity was below 2cm/sec, and the smoothed SWR envelope stayed above 3 standard deviations of the mean for at least 15 ms on at least one tetrode. The full SWR events included times immediately before and after the triggering event during which the envelope exceeded the mean. Replay can only be detected if a sufficient number of cells are simultaneously active, so candidate replay events were defined as sharp waves during which at least 5 place cells from the replayed environment each fired at least one spike.

For visualization each activated place cell was order by the distance of its place field peak (the location at which the cell's occupancy normalized firing rate was greatest)

to the reward location on the center arm of the environment. To determine whether or not a replay event was statistically unlikely to happen by chance, we decoded each candidate event using a Bayesian decoding algorithm. Each event was divided into 15ms bins, and for each bin we calculated the spatial probability distribution:

$$P(X \mid N) = \frac{P(N \mid X)P(X)}{P(N)},$$

where X is the set of all locations in the environment (using 2 cm bins), and N is the list of firing rates for all place cells during the 15ms time bin. $P(N \mid X)$ was calculated using the occupancy normalized rate maps of each place cell, combined with the approximation that spike intervals are Poisson distributed. $P(X)$ was a uniform and uninformative prior which was a flat distribution across all spatial bins. $P(N)$ was not estimated but instead was set to 1 and $P(X \mid N)$ was normalized across X to sum to 1.

To determine if a given decoded sequence was unlikely to occur by chance we drew 10,000 random samples from the $P(X \mid N)$ distribution for each decoded bin and assigned the sample locations to the time of the bin. We then performed a linear regression on the sampled time vs. location points. The resulting R^2 value was then compared to 10,000 regressions where the order of the time bins were shuffled. If the R^2 value was greater than 95% of the R^2 values resulting from shuffling, the event was deemed significantly unlikely to occur by chance.

We also developed a pair-wise measure of replay that is less affected by the number of simultaneously recorded neurons as compared to decoding or previously used statistical tests. To do so we measured, for every pair of cells, the absolute value of the time from each reference spike of one cell to all spikes from the other cell. Only spikes

within SWRs were included. We restricted the time axis to values between 0 and 500 ms and plotted each measured lag between spikes from two cells against the linear distance between the place field centers of the two cells. The linear distance between the place field peaks of the two neurons was measured as the shortest path on the environment from the peak location for one cell to the peak location for the other cell. Each pair of cells was used only once, but all pairs from a given set of SWRs were included in the plot. We then calculated the R^2 value of a linear fit to the points in the plot, which measured the degree to which the time between the spikes could be used to predict the distance between a pair of neuron's place fields.

We also developed a plot to illustrate the quality of pair-wise reactivation based a method used by Euston et. al.[66]. We first computed the cross-correlation histogram between all pairs of neurons with place fields in the environment. This histogram had a bin size of 5 ms and extended from -500 ms to 500 ms from the time of the spike of the second neuron in each pair. We constructed a two dimensional histogram plot where the time between spikes was on the x axis and the counts from each cross correlation histogram were a row placed at the distance between the centers of the two place fields. Thus, the correlegram for a pair of cells with identical place field peak locations would be at the bottom of the plot at a y-value of zero, while the correlegram from two cells whose fields were 50 cm apart would be a row of values at a y-value of 50. Each row was normalized so that the peak and trough ranged from 0 to 1.

The similarity of spatial coding for single cells across the two environments was computed using place field overlap, defined as two times the sum of the overlapping

areas of the linear rate curves divided by the sum of the areas of each curve [45]. This measure is bounded between 0 and 1, where 1 signifies perfect overlap.

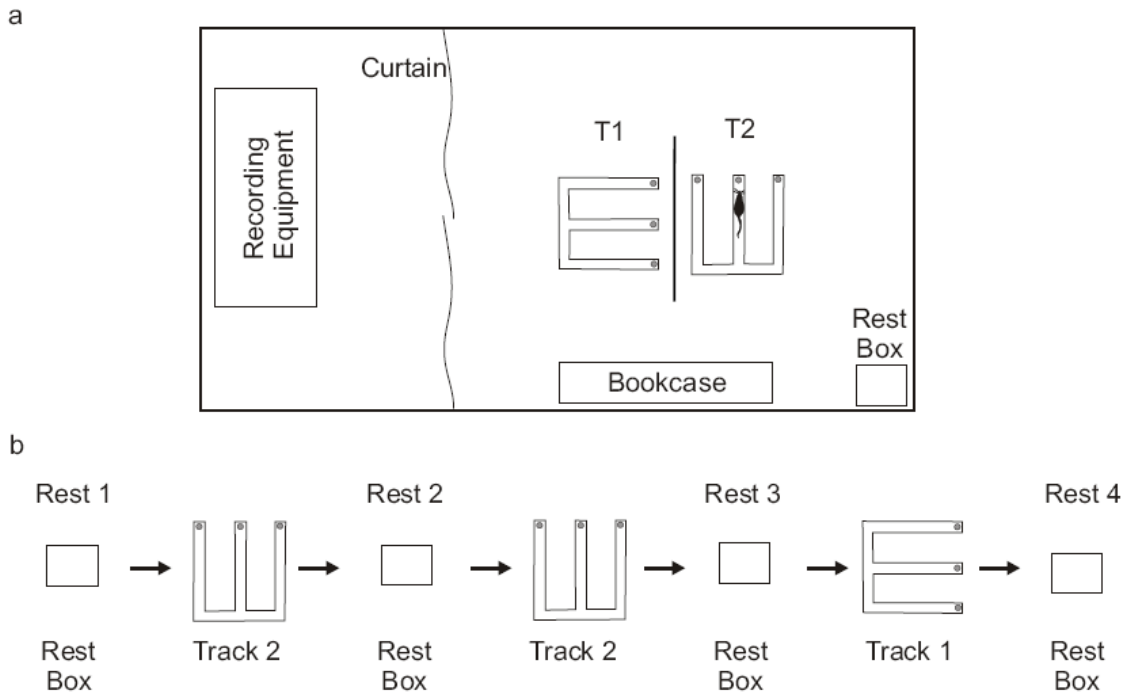


Figure 1. Overview of experimental design. a. Layout of recording room. The region visible to the rat was approximately 3 m square and had a number of prominent visual cues, including the rest box, the curtain and a bookcase. The two tracks were separated by a high barrier, so one track was not visible from the other. The total size of each W-track was 76 cm square, and width of the arms was 7 cm. The rest box was 25 x 34 cm. b. Order of exposures. Each day of recording consisted of two 15 minutes exposures to Track 2 and one 15 minutes exposure to Track 1, and each exposure was flanked by 20 minute rest sessions in a the rest box.

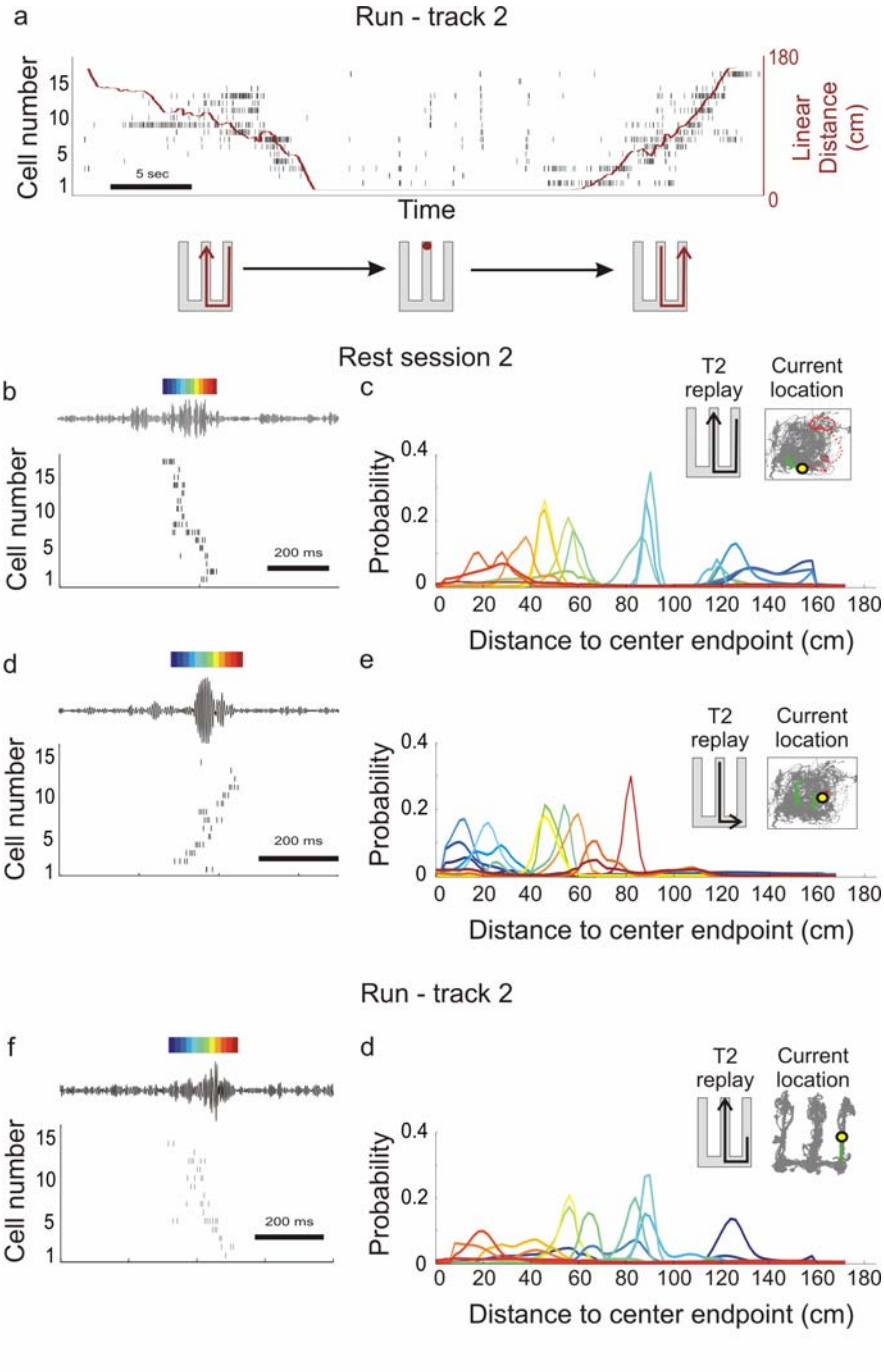


Figure 2. Spatially remote replay in awake periods. a. Spike rasters from one run in T2 where the animal began in the right arm and ended in the center arm. Neurons were ordered as a function of distance from the end of the center arm, and the progression of spatially tuned activity is clearly visible. b. Sequential spiking during SWR while the

animal was awake in the rest box. The bottom plot shows the rasters of all cells that had place fields in T2 and were activated during the SWR. The cells are ordered by the distance of their place field centers from the end of the center arm of T2. The top trace shows the filtered LFP trace taken from one tetrode. The color bar on top of the trace shows the colors associated with the decoding windows used in c. c. Bayesian decoding of location from SRW spiking. Each colored line shows the probability distribution (pdf) resulting from decoding the associated 15 ms period from b. The cartoon of E1 shows the trajectory that was replayed and the diagram of the rest box shows the recent history of the animal's motion in the rest box. Gray dots represent all sample locations, red dots represent the locations the animal was in during the five seconds before the SWR, the black circle represents the animal's location during the SWR, and the green dots represent the animal's location in the five seconds following the SWR. The replayed event extends from the end of the right arm to the end of the center arm. d, e. A second example of replay, where the event begins in the center arm and extends toward the left arm. All panels are as described for b. and c. above. f, g. A reference replay event similar to that shown in b. and c. from a time when the animal was in T2. This event originated at the animal's location on the track as can be seen from the current location plot in the upper right of g.

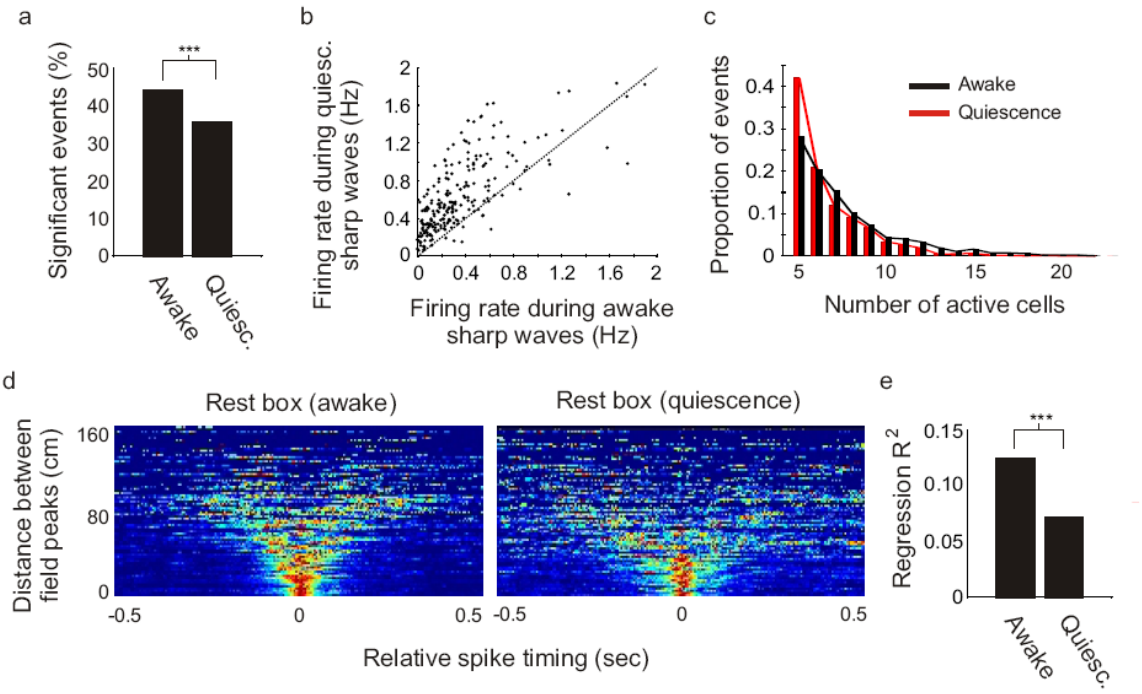


Figure 3. Replay of T2 in the rest box is more robust during awake as compared to quiescent periods. a. The proportion of significant replay events was significantly higher during awake periods ($p < 0.001$), even when quiescent periods were defined as periods of immobility for as little as five seconds. b. Scatter plot of the firing rate of all neurons with place fields in T2 during awake and quiescent SWRs in the rest box. Rates for the large majority of neurons were higher during quiescence ($p < 10^{-10}$). c. Histogram of the proportions of SWRs during awake and quiescent periods with different numbers of cells active. Awake SWRs were more likely to activate 7 or more cells while quiescent SWRs were more likely to activate 5 or 6 cells ($p < 10^{-10}$). d. Pair-wise reactivation in the rest box. Each plot shows rows representing the normalized cross-correlegrams between all pairs of simultaneously recorded neurons with place fields in T2, with the vertical location of each row determined by the distance between the two cells place field peaks in E1. The 'V' representing activation consistent with replay is more clearly visible in

the awake state. e. Pair-wise reactivation in the rest box was more stronger during awake periods. The R^2 value represents the degree to which the times between spikes from two neurons predict the distances between the peaks of their place fields, and was significantly larger for awake replay events ($p < 10^{-10}$).

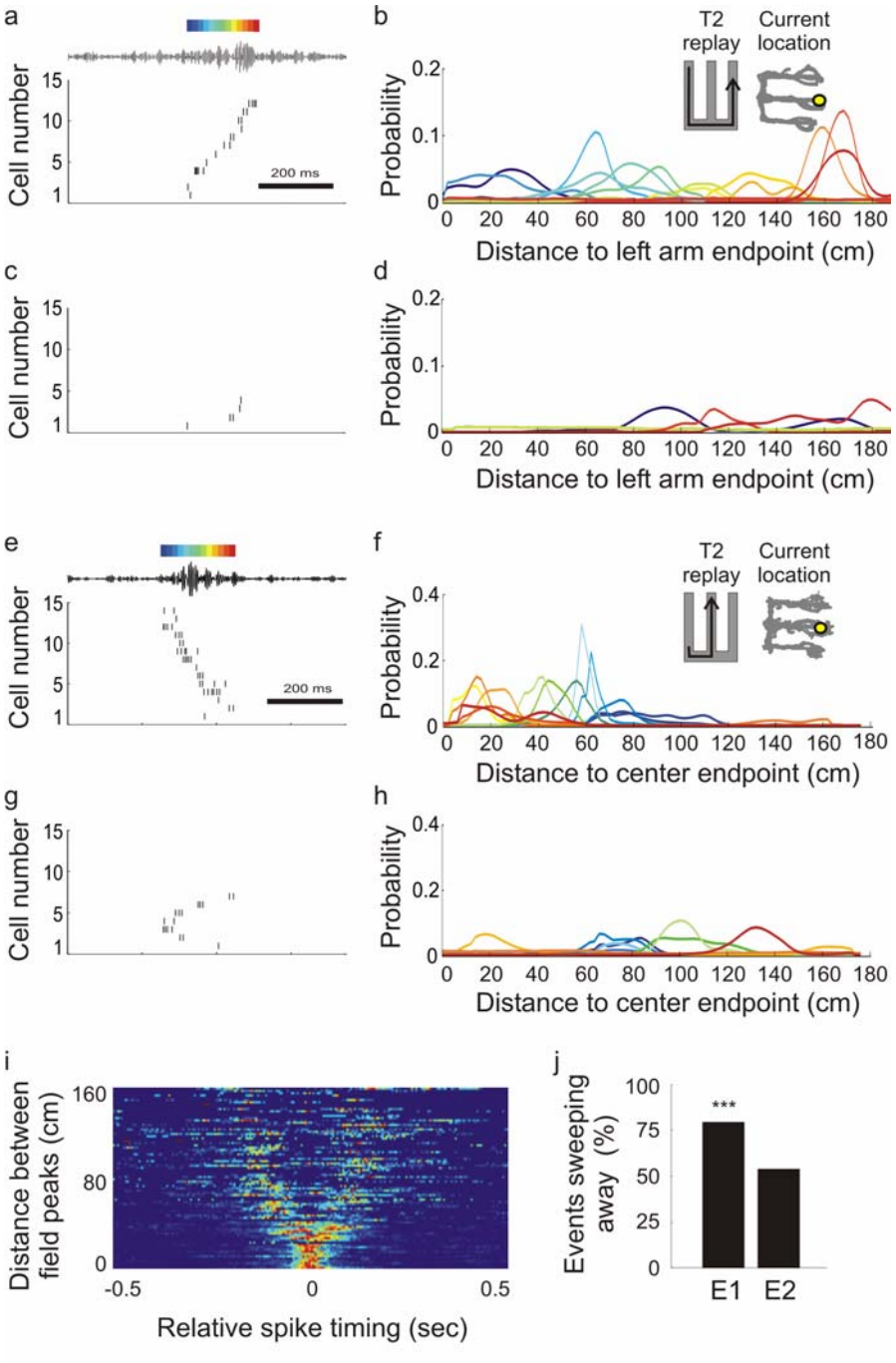


Figure 4. Robust replay of T2 while the animal was located in T1. a, b. Sequential activation of neurons representing a coherent spatial sequence in E1. See Fig. 2 for a detailed description of each element of the plots. Note that this is not a sequence for which the animal would have received a reward during the performance of the task.

c, d. Activation of neurons with place fields in T1 during the same SWR event and the decoded sequence for E2. The neural activity during the SWR involved a coherent replay of T2 but not of T1. Note, cell numbers in a do not correspond to cell numbers in c, as different sets of cells were active in the two tracks. e, f, g, h. A second example illustrating replay of T2 in the absence of replay of T1. i. Pair-wise correlation plot for T1 SWRs including only neurons with place fields in T2 but not in T1. The 'V' representing coherent replay is clearly visible when cells with place fields in the current environment are excluded.

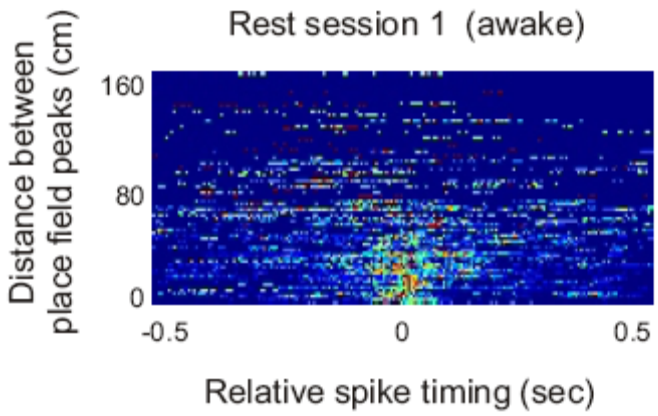


Figure 5. No evidence for replay before the exposures to T2 and T1 during the first rest session of the day. See Fig. 2d for a detailed explanation of the composition of the plot. There was some evidence for co-firing of cells with overlapping place fields as illustrated by the red region near 0, 0, but there was no evidence for coherent sequential replay.

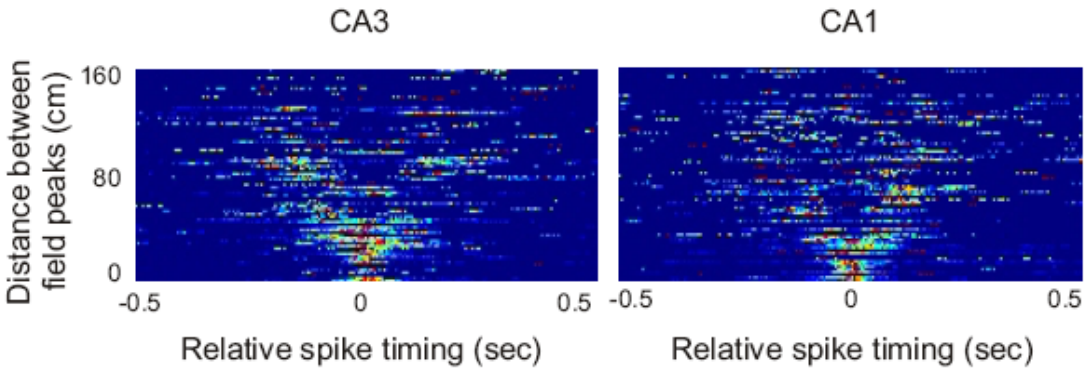
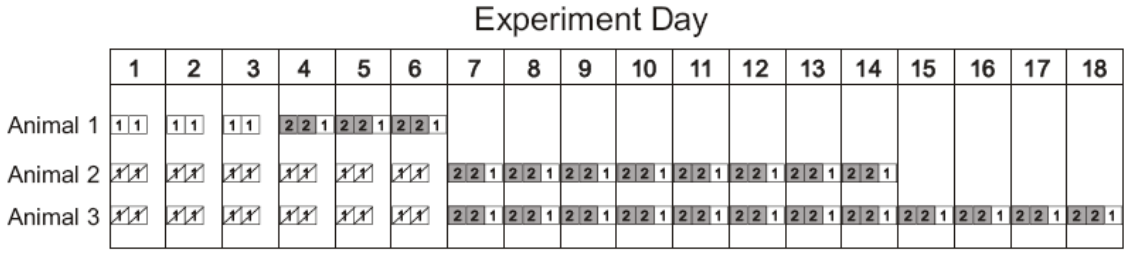
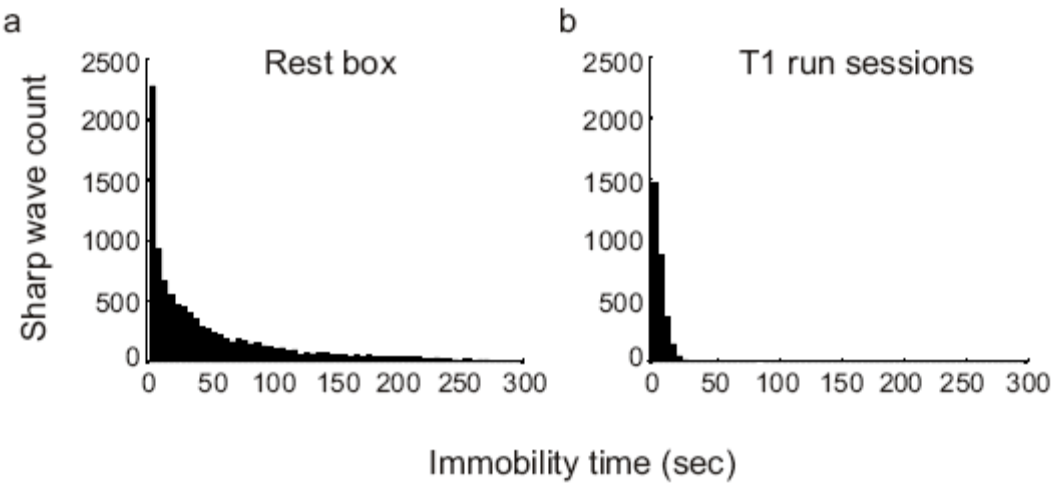


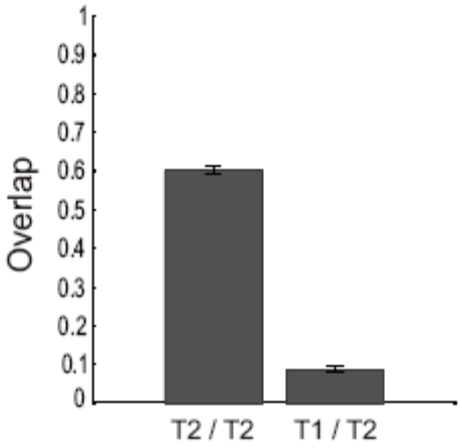
Figure 6. Evidence for replay in CA3 and CA1 individually. a. Pair-wise normalized cross-correlegram plot for CA3. b. Pair-wise normalized cross-correlegram plot for CA1. The 'V' indicating replay is clearly evident for both populations.



Supplemental Figure 1. Recording schedule for each animal across days. White squares indicate a 15 minute run on Track 1. Gray squares represent a run on Track 2. Squares with a diagonal line represent days when neural data were not collected.



Supplementary Figure 2. Histogram of lengths of immobility periods for each SWR event. Left: Histogram of lengths for the Rest box. Right: Histogram of lengths for T1 run sessions. We measured the length of the immobility period up to the time of each SWR event and generated histograms for that set of times using 5 ms bins. These histograms show that animals were frequently stationary for long periods of time in the rest box but were rarely stationary for more than 20 seconds during the run in T1.



Supplementary Figure 3. Place field overlap for T2 and T1. The left bar shows the mean ± SEM for the place field overlap for individual place fields taken from the first and second runs on each day in T2. The relatively high overlap indicates that place fields were generally stable across runs. The right bar show the place field overlap for the place fields from cells that had fields on either T1 or T2 or both. The low overlap indicates that the animals formed distinct spatial representations for the two tracks.

Notes

1. Scoville,W.B. & Milner,B. Loss of recent memory after bilateral hippocampal lesions. *J. Neurol. Neurosurg. Psychiatry* **20**, 11-21 (1957).

2. O'Keefe,J. & Nadel,L. *The hippocampus as a cognitive map*(Oxford University Press, London, 1978).

3. Squire,L.R. & Zola-Morgan,S. The neuropsychology of memory: new links between humans and experimental animals. *Ann. N. Y. Acad. Sci.* **444:137-49**, 137-149 (1985).

4. Morris,R.G., Garrud,P., Rawlins,J.N., & O'Keefe,J. Place navigation impaired in rats with hippocampal lesions. *Nature* **297**, 681-683 (1982).

5. Jarrard,L.E. On the role of the hippocampus in learning and memory in the rat. *Behav. Neural Biol.* **60**, 9-26 (1993).

6. O'Keefe,J. & Dostrovsky,J. The hippocampus as a spatial map. Preliminary evidence from unit activity in the freely-moving rat. *Brain Res.* **34**, 171-175 (1971).

7. Muller,R. A quarter of a century of place cells. *Neuron* **17**, 813-822 (1996).

8. Wilson,M.A. & McNaughton,B.L. Dynamics of the hippocampal ensemble code for space. *Science* **261**, 1055-1058 (1993).

9. Frank,L.M., Stanley,G.B., & Brown,E.N. Hippocampal plasticity across multiple days of exposure to novel environments. *J. Neurosci.* **24**, 7681-7689 (2004).

10. Lee,I. & Kesner,R.P. Differential roles of dorsal hippocampal subregions in spatial working memory with short versus intermediate delay. *Behav. Neurosci.* **117**, 1044-1053 (2003).

11. Nakazawa,K. *et al.* Hippocampal CA3 NMDA receptors are crucial for memory acquisition of one-time experience. *Neuron* **38**, 305-315 (2003).

12. Leutgeb,S., Leutgeb,J.K., Treves,A., Moser,M.B., & Moser,E.I. Distinct ensemble codes in hippocampal areas CA3 and CA1. *Science* **305**, 1295-1298 (2004).

13. Amaral,D.G. & Witter,M.P. The three-dimensional organization of the hippocampal formation: a review of anatomical data. *Neuroscience* **31**, 571-591 (1989).

14. Marr,D. Simple memory: a theory for archicortex. *Philos. Trans. R. Soc. Lond.* **262**, 23-81 (1971).

15. McClelland,J.L., McNaughton,B.L., & O'Reilly,R.C. Why there are complementary learning systems in the hippocampus and neocortex: insights from the successes and failures of connectionist models of learning and memory. *Psychol. Rev.* **102**, 419-457 (1995).

16. Lisman,J.E. Relating hippocampal circuitry to function: recall of memory sequences by reciprocal dentate-CA3 interactions. *Neuron* **22**, 233-242 (1999).

17. Kali,S. & Dayan,P. The involvement of recurrent connections in area CA3 in establishing the properties of place fields: a model. *J. Neurosci.* **20**, 7463-7477 (2000).

18. Jensen,O. & Lisman,J.E. Hippocampal CA3 region predicts memory sequences: accounting for the phase precession of place cells. *Learn. Mem.* **3**, 279-287 (1996).

19. Squire,L.R. & Zola-Morgan,S. The medial temporal lobe memory system. *Science* **253**, 1380-1386 (1991).

20. Eichenbaum,H. & Cohen,N.J. *From Conditioning to Conscious Recollection*(Oxford University Press, New York, 2001).

21. Best,P.J., White,A.M., & Minai,A. Spatial processing in the brain: the activity of hippocampal place cells. *Annu. Rev. Neurosci.* **24:459-86.**, 459-486 (2001).

22. Lee,I., Yoganarasimha,D., Rao,G., & Knierim,J.J. Comparison of population coherence of place cells in hippocampal subfields CA1 and CA3. *Nature* **430**, 456-459 (2004).

23. Knight,R. Contribution of human hippocampal region to novelty detection. *Nature.* **19;383**, 256-259 (1996).

24. Knight,R.T. & Nakada,T. Cortico-limbic circuits and novelty: a review of EEG and blood flow data. *Rev. Neurosci.* **9**, 57-70 (1998).

25. Kirchhoff,B.A., Wagner,A.D., Maril,A., & Stern,C.E. Prefrontal-temporal circuitry for episodic encoding and subsequent memory. *J. Neurosci.* **20**, 6173-6180 (2000).

26. Li,L., Miller,E.K., & Desimone,R. The representation of stimulus familiarity in anterior inferior temporal cortex. *J. Neurophysiol.* **69**, 1918-1929 (1993).

27. Nitz,D. & McNaughton,B. Differential modulation of CA1 and dentate gyrus interneurons during exploration of novel environments. *J. Neurophysiol.* **91**, 863-872 (2004).

28. Csicsvari,J., O'Neill,J., Allen,K., & Senior,T. Place-selective firing contributes to the reverse-order reactivation of CA1 pyramidal cells during sharp waves in open-field exploration. *Eur. J. Neurosci.* **26**, 704-716 (2007).

29. Guzowski,J.F., Knierim,J.J., & Moser,E.I. Ensemble dynamics of hippocampal regions CA3 and CA1. *Neuron* **44**, 581-584 (2004).

30. Lee,I., Rao,G., & Knierim,J.J. A double dissociation between hippocampal subfields: differential time course of CA3 and CA1 place cells for processing changed environments. *Neuron* **42**, 803-815 (2004).

31. Frank,L.M., Brown,E.N., & Wilson,M.A. Trajectory encoding in the hippocampus and entorhinal cortex. *Neuron* **27**, 169-178 (2000).

32. Tanila,H. Hippocampal place cells can develop distinct representations of two visually identical environments. *Hippocampus.* **9**, 235-246 (1999).

33. McNaughton,B.L., Barnes,C.A., & O'Keefe,J. The contributions of position, direction, and velocity to single unit activity in the hippocampus of freely-moving rats. *Exp. Brain Res.* **52**, 41-49 (1983).

34. Lever,C., Wills,T., Cacucci,F., Burgess,N., & O'Keefe,J. Long-term plasticity in hippocampal place-cell representation of environmental geometry. *Nature* **416**, 90-94 (2002).

35. Hensch,T.K. Critical period regulation. *Annu. Rev. Neurosci.* **27:549-79.**, 549-579 (2004).

36. Han,J.H. *et al.* Neuronal competition and selection during memory formation. *Science.* **20;316**, 457-460 (2007).

37. Hardingham,G.E., Arnold,F.J., & Bading,H. Nuclear calcium signaling controls CREB-mediated gene expression triggered by synaptic activity. *Nat. Neurosci.* **4**, 261-267 (2001).

38. Laughlin,S.B., de Ruyter van Steveninck RR, & Anderson,J.C. The metabolic cost of neural information. *Nat. Neurosci.* **1**, 36-41 (1998).

39. Lisman,J.E. & Otmakhova,N.A. Storage, recall, and novelty detection of sequences by the hippocampus: elaborating on the SOCRATIC model to account for normal and aberrant effects of dopamine. *Hippocampus* **11**, 551-568 (2001).

40. Kumaran,D. & Maguire,E.A. Match mismatch processes underlie human hippocampal responses to associative novelty. *J. Neurosci.* **27**, 8517-8524 (2007).

41. Kumaran,D. & Maguire,E.A. An unexpected sequence of events: mismatch detection in the human hippocampus. *PLoS. Biol.* **4**, e424 (2006).

42. Legault,M. & Wise,R.A. Novelty-evoked elevations of nucleus accumbens dopamine: dependence on impulse flow from the ventral subiculum and glutamatergic neurotransmission in the ventral tegmental area. *Eur. J. Neurosci.* **13**, 819-828 (2001).

43. Buzsaki,G. Hippocampal sharp waves: their origin and significance. *Brain Res.* **398**, 242-252 (1986).

44. Buzsaki,G., Horvath,Z., Urioste,R., Hetke,J., & Wise,K. High-frequency network oscillation in the hippocampus. *Science* **256**, 1025-1027 (1992).

45. Battaglia,F.P., Sutherland,G.R., & McNaughton,B.L. Local sensory cues and place cell directionality: additional evidence of prospective coding in the hippocampus. *J. Neurosci.* **24**, 4541-4550 (2004).

46. Sutherland,G.R. & McNaughton,B. Memory trace reactivation in hippocampal and neocortical neuronal ensembles. *Curr. Opin. Neurobiol.* **10**, 180-186 (2000).

47. Cheng,S. & Frank,L.M. New experiences enhance coordinated neural activity in the hippocampus. *Neuron.* **57**, 303-313 (2008).

48. Suzuki,W.A. Encoding new episodes and making them stick. *Neuron* **50**, 19-21 (2006).

49. Wilson,M.A. & McNaughton,B.L. Reactivation of hippocampal ensemble memories during sleep. *Science* **265**, 676-679 (1994).

50. Chrobak,J.J. & Buzsaki,G. High-frequency oscillations in the output networks of the hippocampal- entorhinal axis of the freely behaving rat. *J. Neurosci.* **16**, 3056-3066 (1996).

51. Csicsvari,J., Hirase,H., Mamiya,A., & Buzsaki,G. Ensemble patterns of hippocampal CA3-CA1 neurons during sharp wave-associated population events. *Neuron* **28**, 585-594 (2000).

52. Pavlides,C. & Winson,J. Influences of hippocampal place cell firing in the awake state on the activity of these cells during subsequent sleep episodes. *J. Neurosci.* **9**, 2907-2918 (1989).

53. Kudrimoti,H.S., Barnes,C.A., & McNaughton,B.L. Reactivation of hippocampal cell assemblies: effects of behavioral state, experience, and EEG dynamics. *J. Neurosci.* **19**, 4090-4101 (1999).

54. O'Neill,J., Senior,T.J., Allen,K., Huxter,J.R., & Csicsvari,J. Reactivation of experience-dependent cell assembly patterns in the hippocampus. *Nat. Neurosci.* **11**, 209-215 (2008).

55. Lee,A.K. & Wilson,M.A. Memory of sequential experience in the hippocampus during slow wave sleep. *Neuron* **36**, 1183-1194 (2002).

56. Ji,D. & Wilson,M.A. Coordinated memory replay in the visual cortex and hippocampus during sleep. *Nat Neurosci* **10**, 100-107 (2007).

57. Csicsvari,J., O'Neill,J., Allen,K., & Senior,T. Place-selective firing contributes to the reverse-order reactivation of CA1 pyramidal cells during sharp waves in open-field exploration. *Eur. J Neurosci* **26**, 704-716 (2007).

58. Nadasdy,Z., Hirase,H., Czurko,A., Csicsvari,J., & Buzsaki,G. Replay and time compression of recurring spike sequences in the hippocampus. *J. Neurosci.* **19**, 9497-9507 (1999).

59. Stickgold,R. Sleep-dependent memory consolidation. *Nature* **437**, 1272-1278 (2005).

60. Rasch,B. & Born,J. Maintaining memories by reactivation. *Curr. Opin. Neurobiol.* **17**, 698-703 (2007).

61. Wagner,U., Hallschmid,M., Rasch,B., & Born,J. Brief sleep after learning keeps emotional memories alive for years. *Biol. Psychiatry* **60**, 788-790 (2006).

62. Foster,D.J. & Wilson,M.A. Reverse replay of behavioural sequences in hippocampal place cells during the awake state. *Nature.* **440**, 680-683 (2006).

63. Diba,K. & Buzsaki,G. Forward and reverse hippocampal place-cell sequences during ripples. *Nat. Neurosci.* **10**, 1241-1242 (2007).

64. O'Neill,J., Senior,T., & Csicsvari,J. Place-selective firing of CA1 pyramidal cells during sharp wave/ripple network patterns in exploratory behavior. *Neuron* **49**, 143-155 (2006).

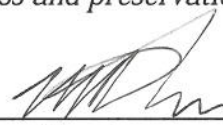
65. O'Neill,J., Senior,T.J., Allen,K., Huxter,J.R., & Csicsvari,J. Reactivation of experience-dependent cell assembly patterns in the hippocampus. *Nat. Neurosci.* **11**, 209-215 (2008).

66. Euston,D.R., Tatsuno,M., & McNaughton,B.L. Fast-forward playback of recent memory sequences in prefrontal cortex during sleep. *Science.* **318**, 1147-1150 (2007).

Publishing Agreement

It is the policy of the University to encourage the distribution of all theses and dissertations. Copies of all UCSF theses and dissertations will be routed to the library via the Graduate Division. The library will make all theses and dissertations accessible to the public and will preserve these to the best of their abilities, in perpetuity.

Please sign the following statement:
I hereby grant permission to the Graduate Division of the University of California, San Francisco to release copies of my thesis or dissertation to the Campus Library to provide access and preservation, in whole or in part, in perpetuity.



Author Signature

9/8/08

Date